Workshop “Innovation in engineering design”

29 - 30 November 2010, Kragujevac

M5 computations in production engineering and technologie

Tomaž Rodič

Faculty of Natural Sciences and Engineering

University of Ljubljana

Name/s of presenter/s

This project has been funded with support from the European Commission

M5 application areas

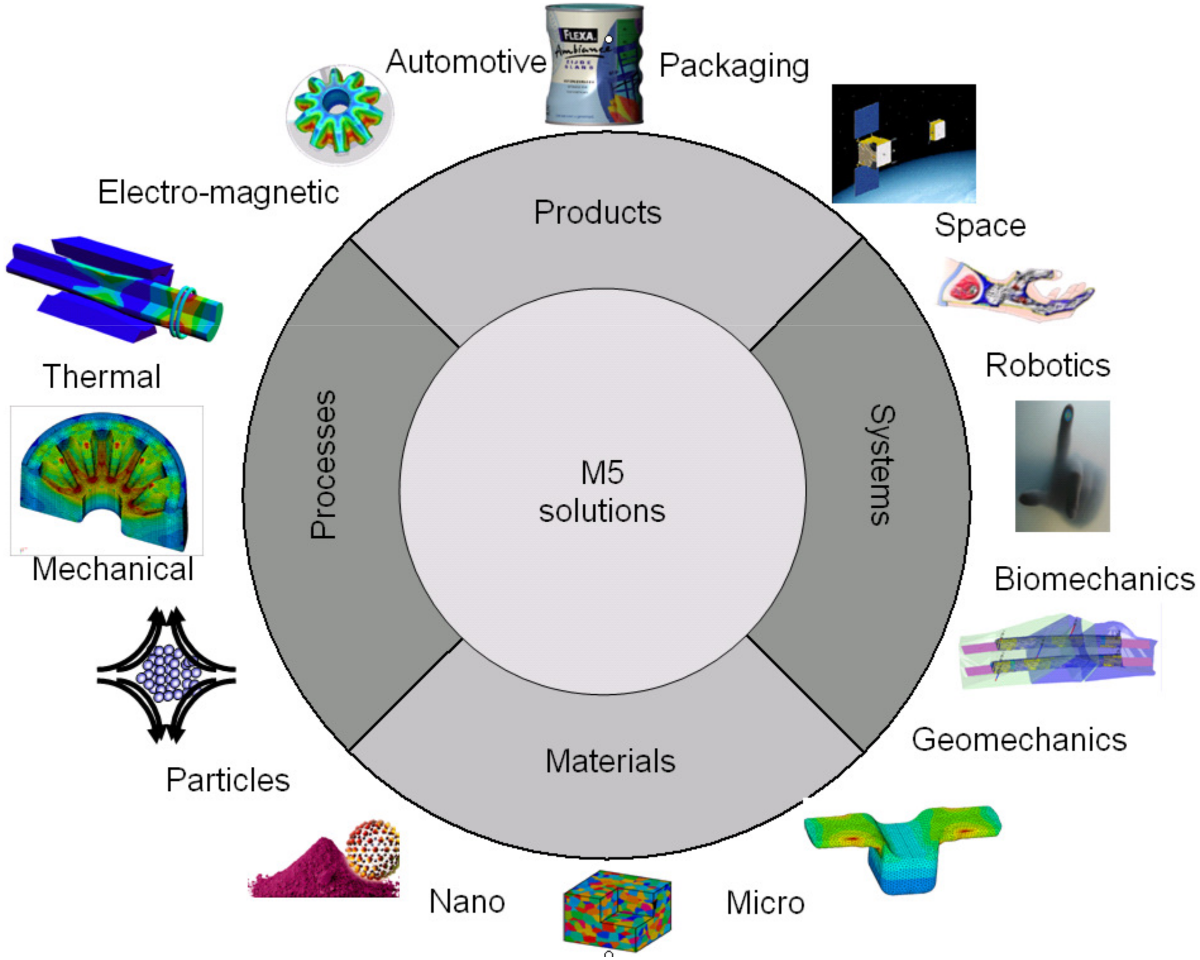

M5: Multi-field, Multi-scale, Multi-body, Multi-phase, Multi-objective

Multi-field

Multi-scale

Multi-body

Multi-phase

Multi-objective

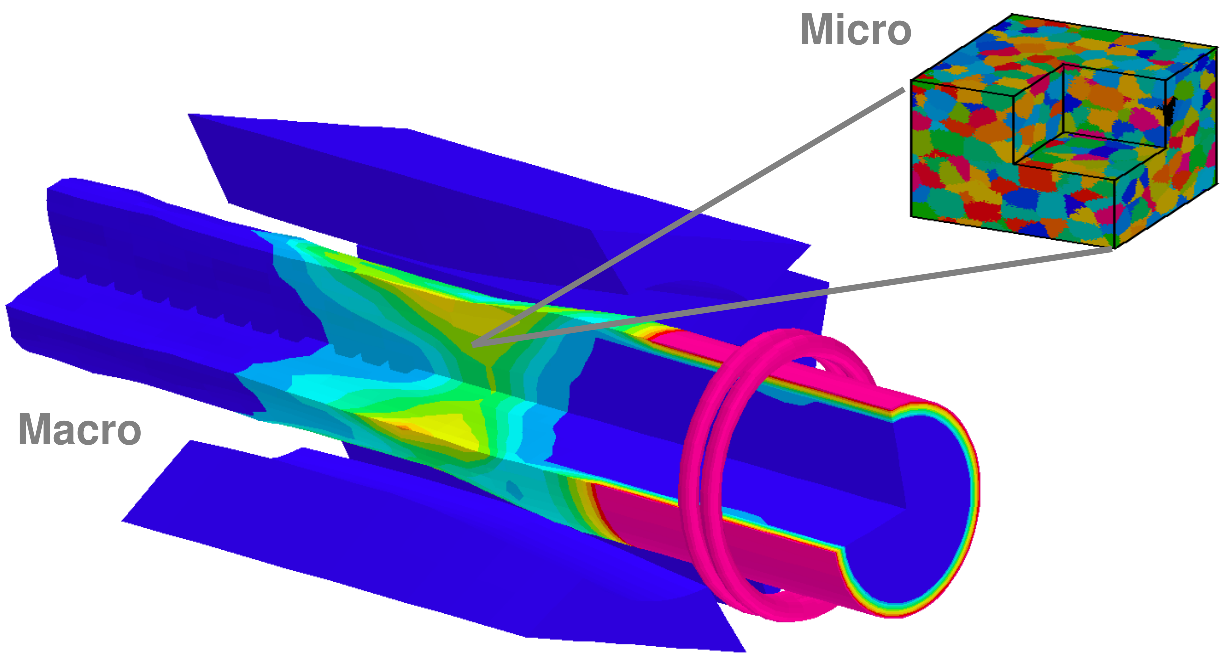

Multi-field problems

Coupled analyses of mechanical – thermal - magnetic fields when combining radial forging with inductive heating

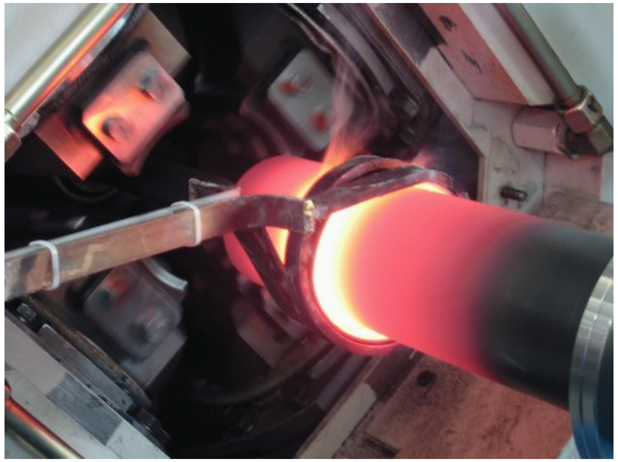

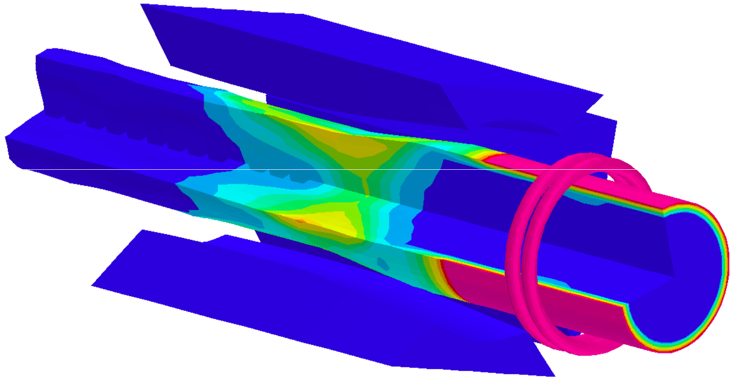

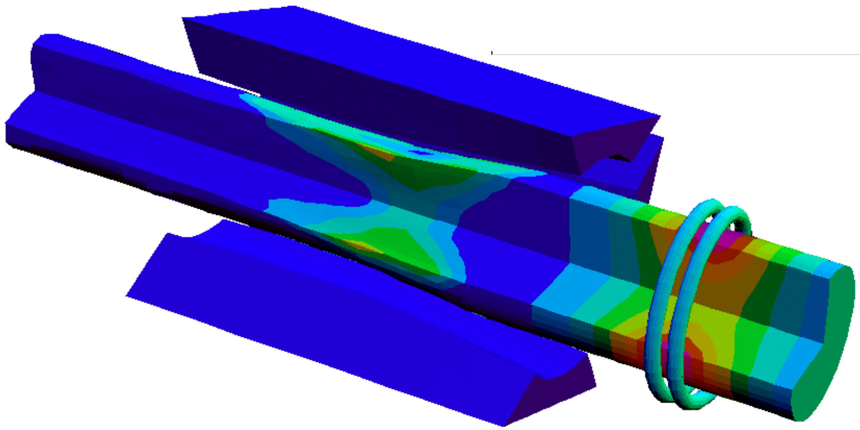

Coupled Macro – Micro analysis

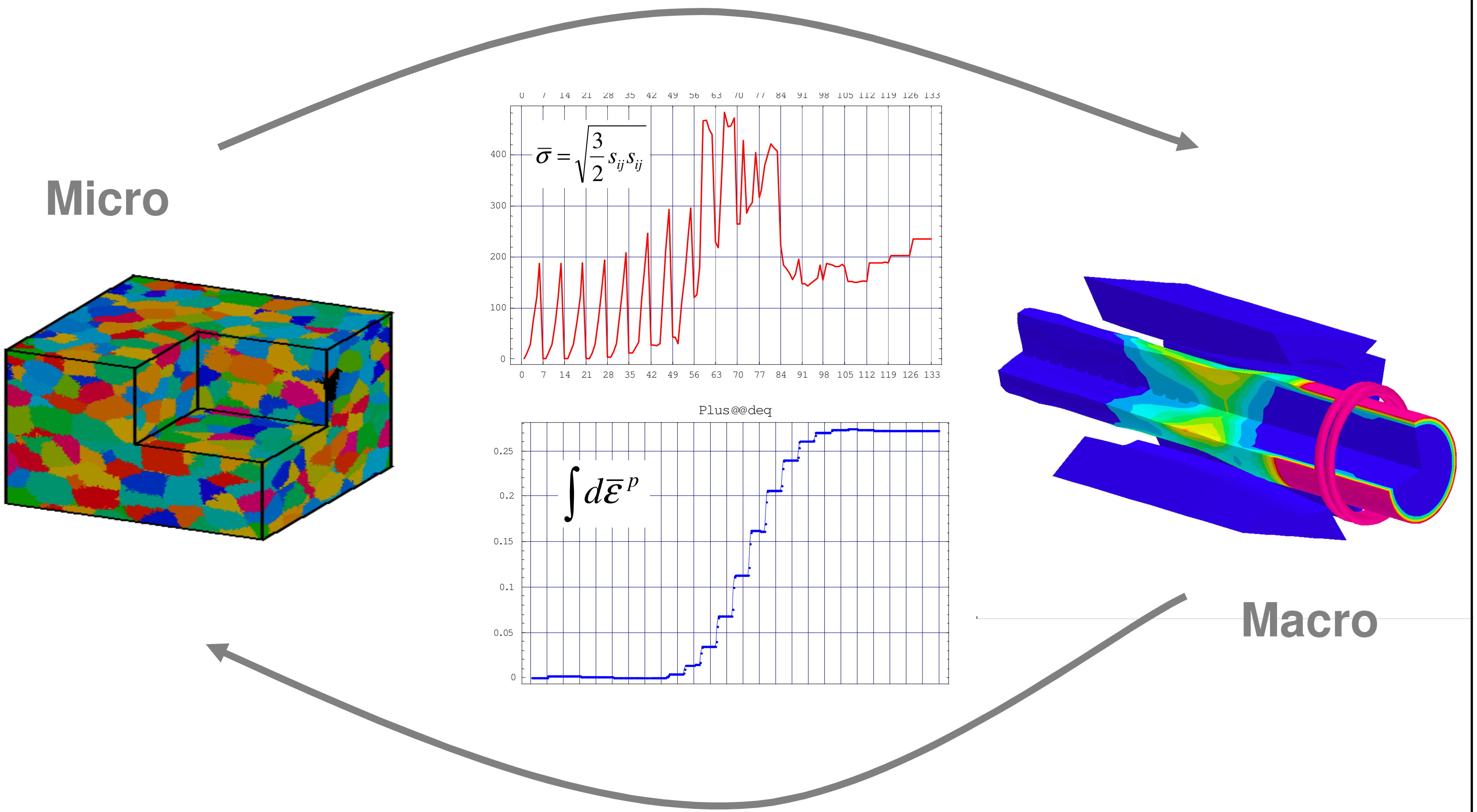

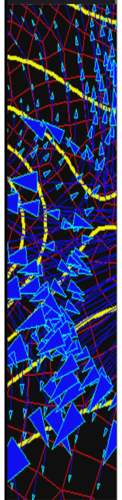

METAL RAVNE

Radial forging

GFM

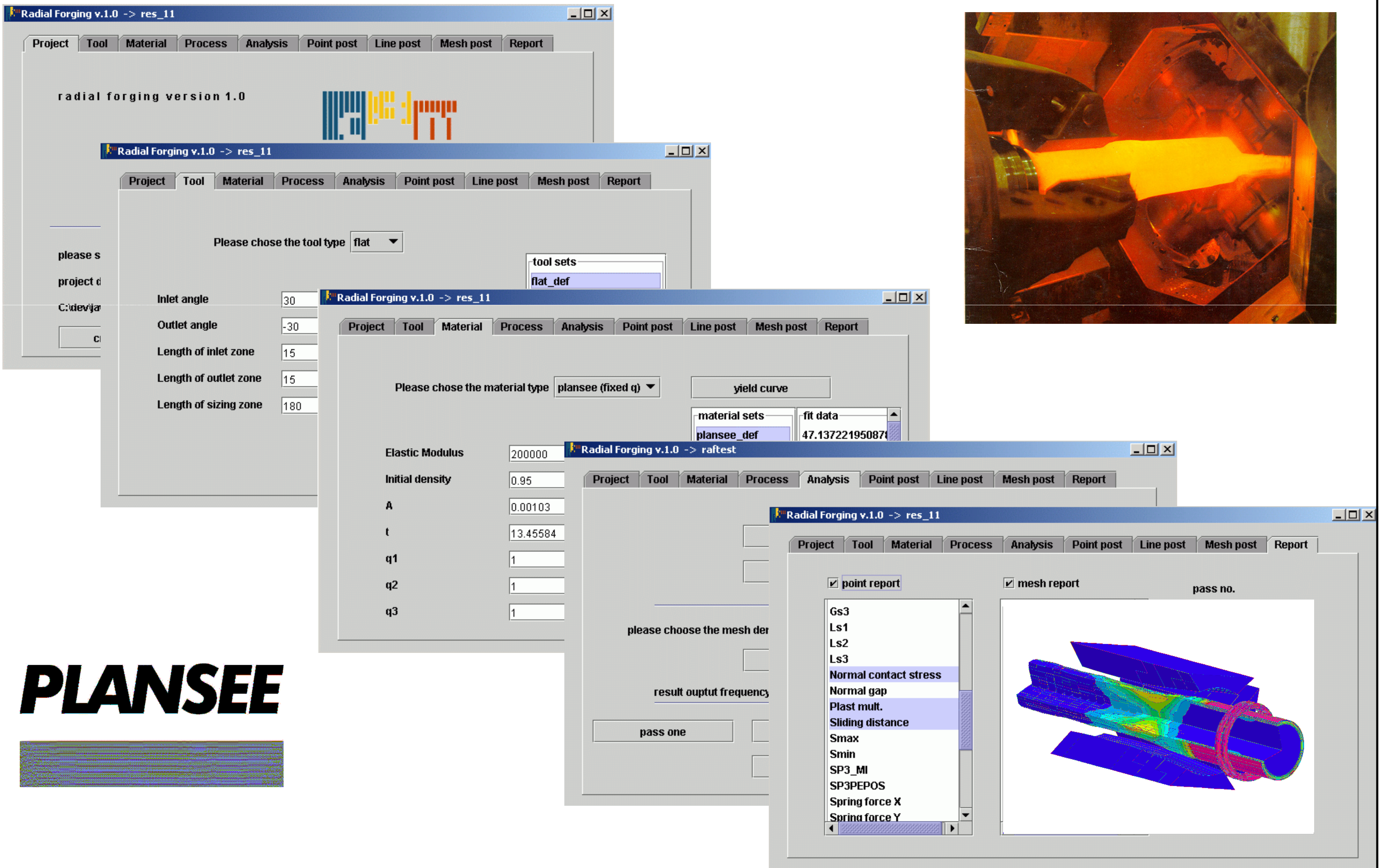

PLANSEE

Real and virtual process simulations

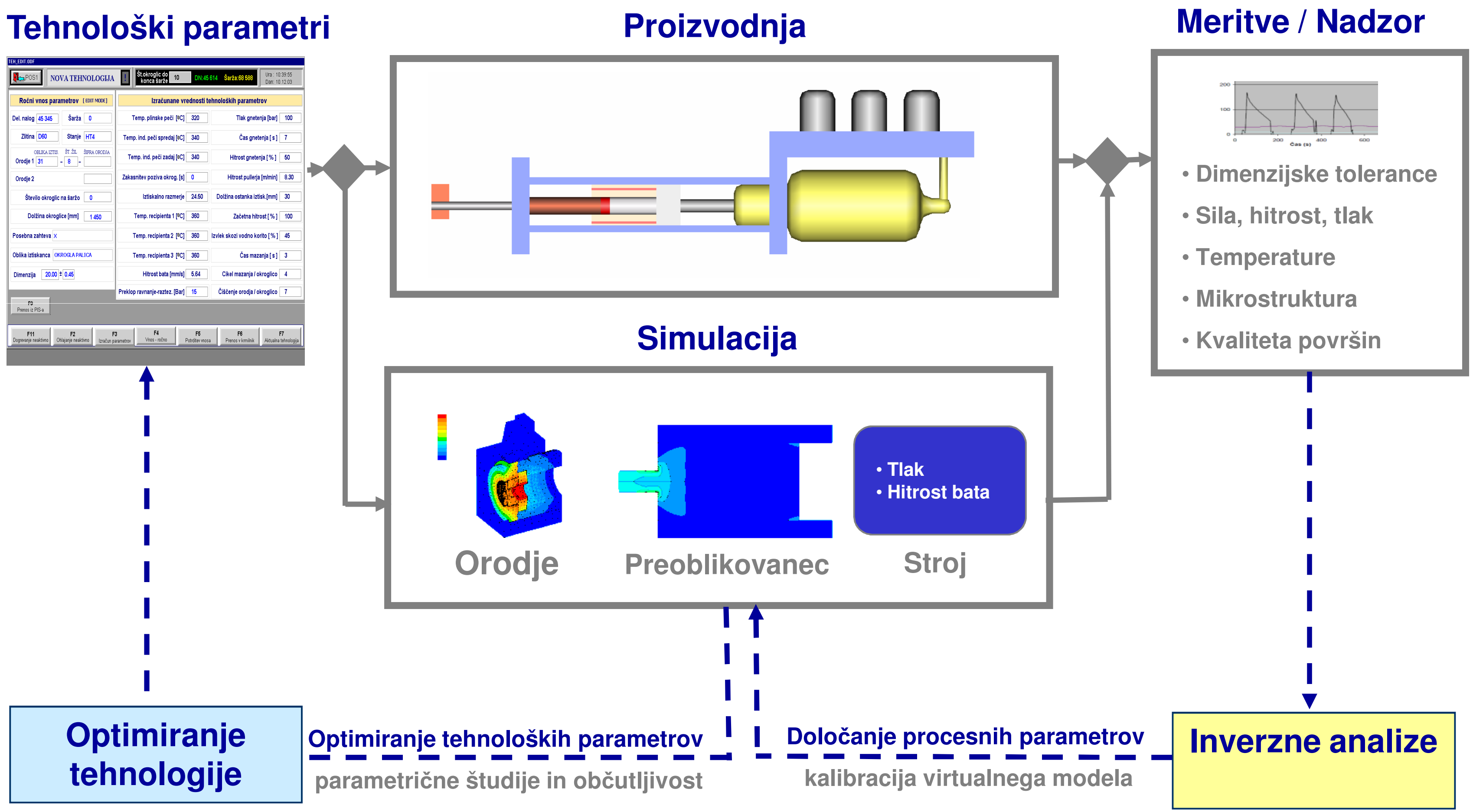

Cold precision forming

Damage at macro & micro scales

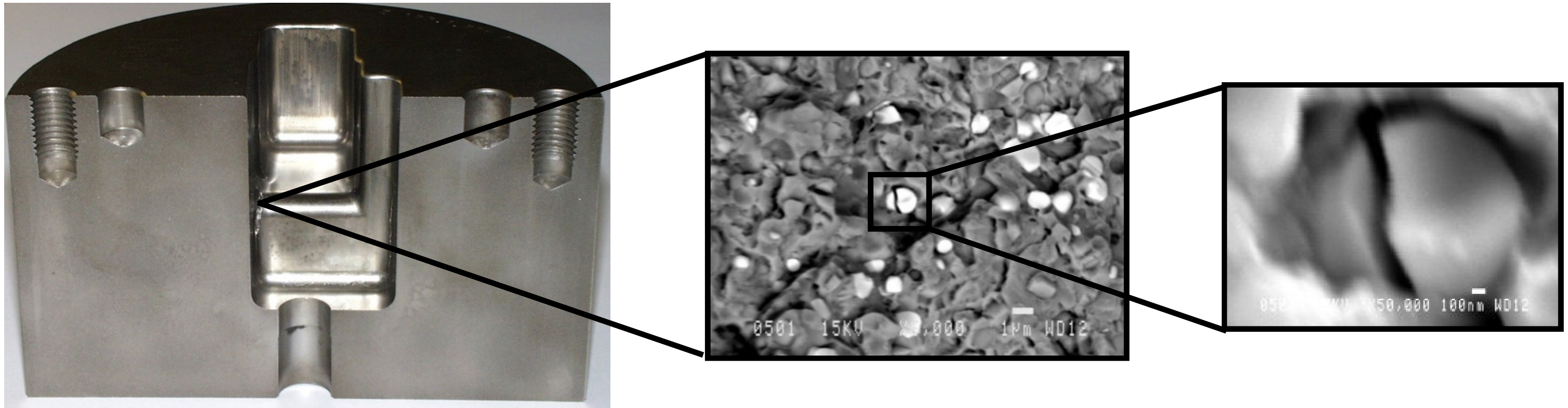

Damage at macro & micro scales

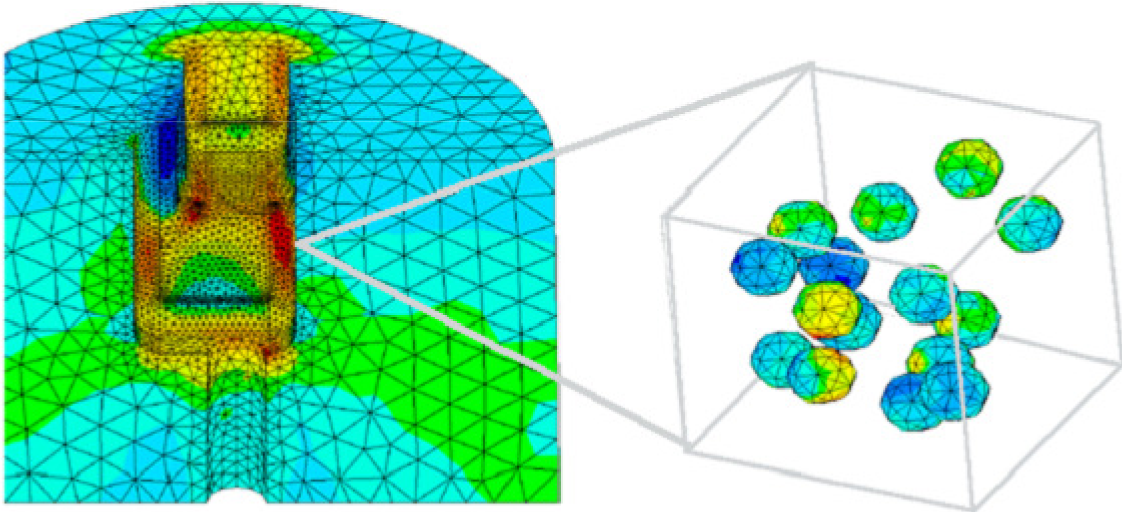

Press deflections

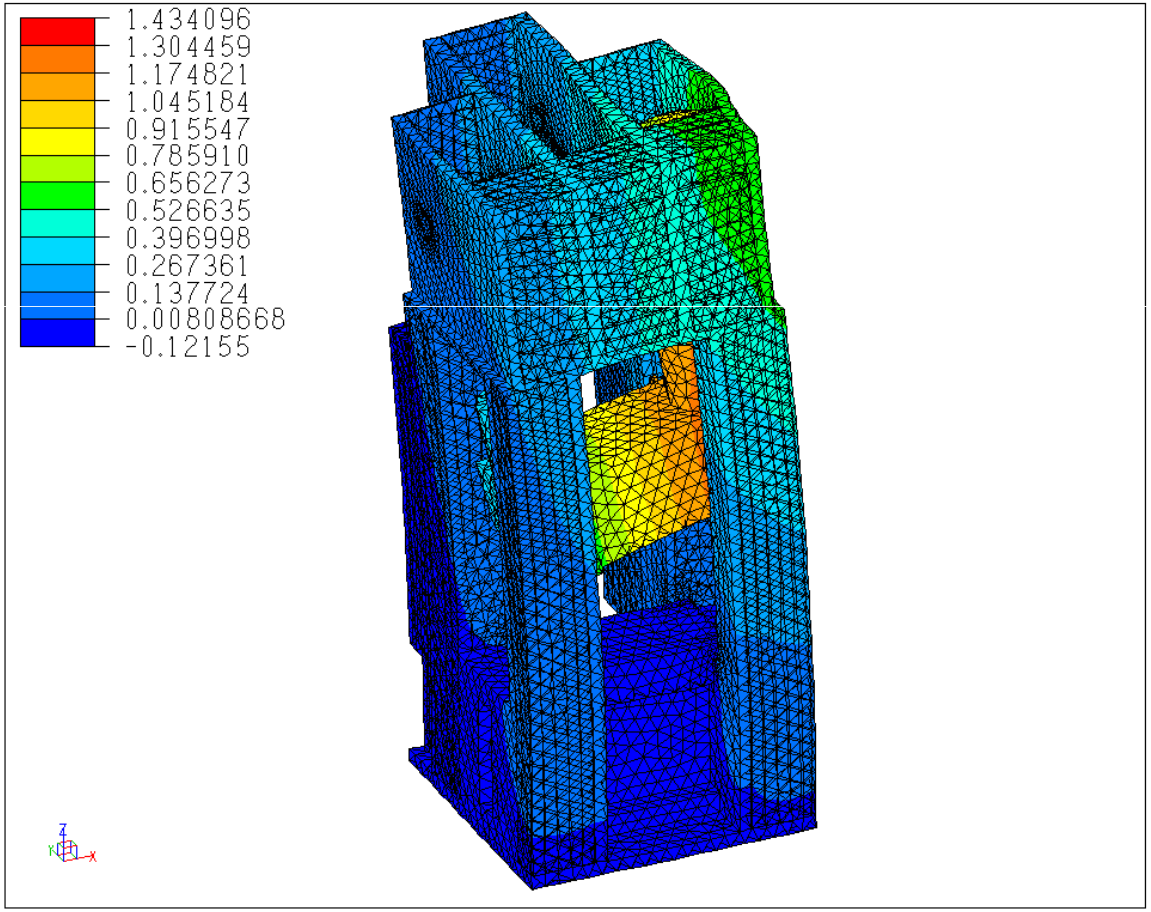

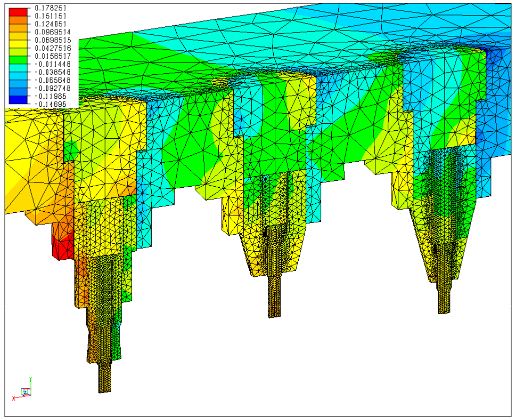

Eccentric load in multistage

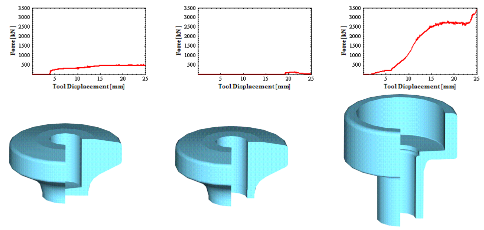

Stochastic interactions

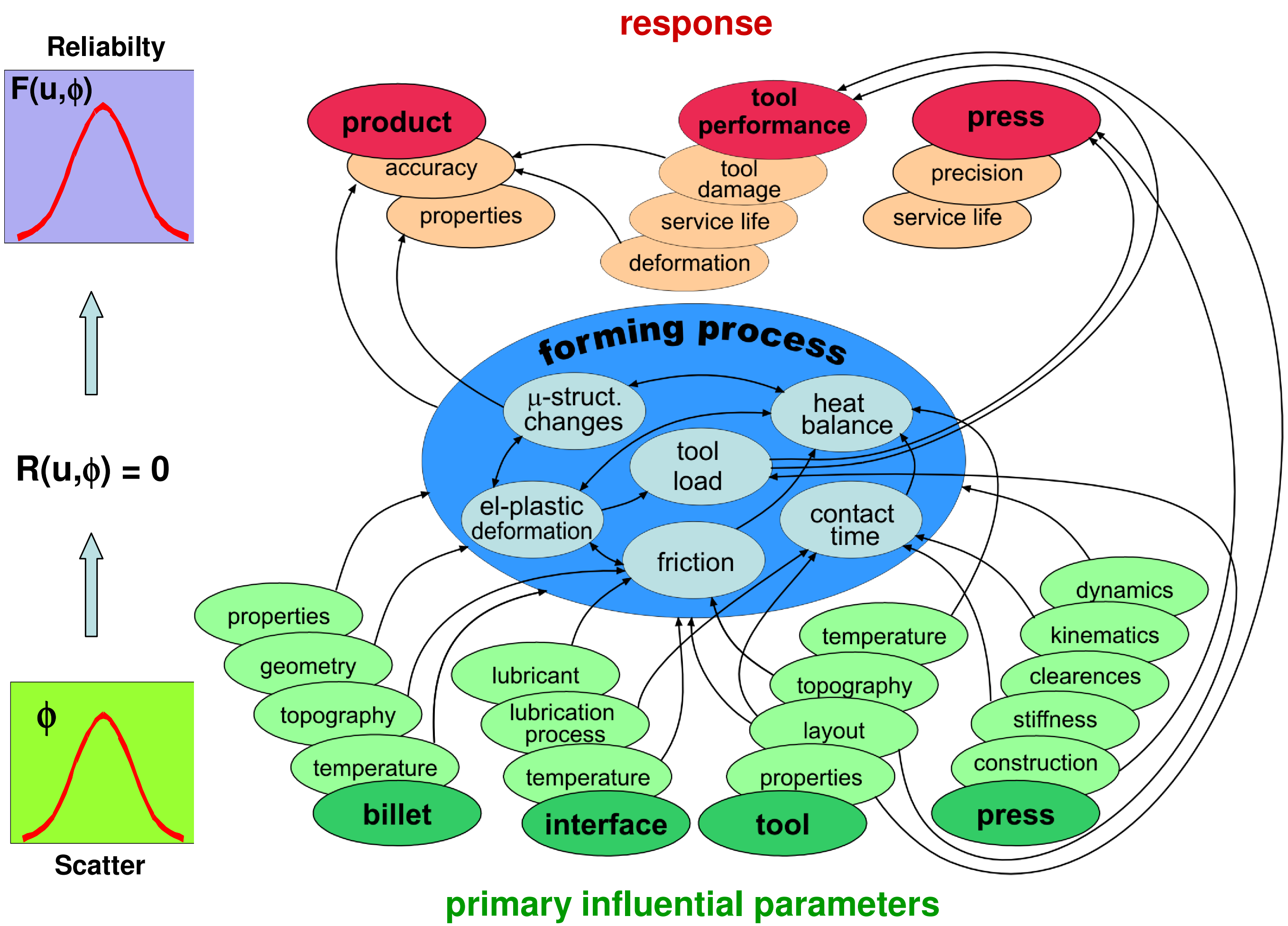

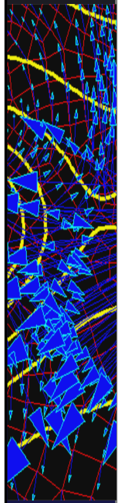

Code development system

AceGen

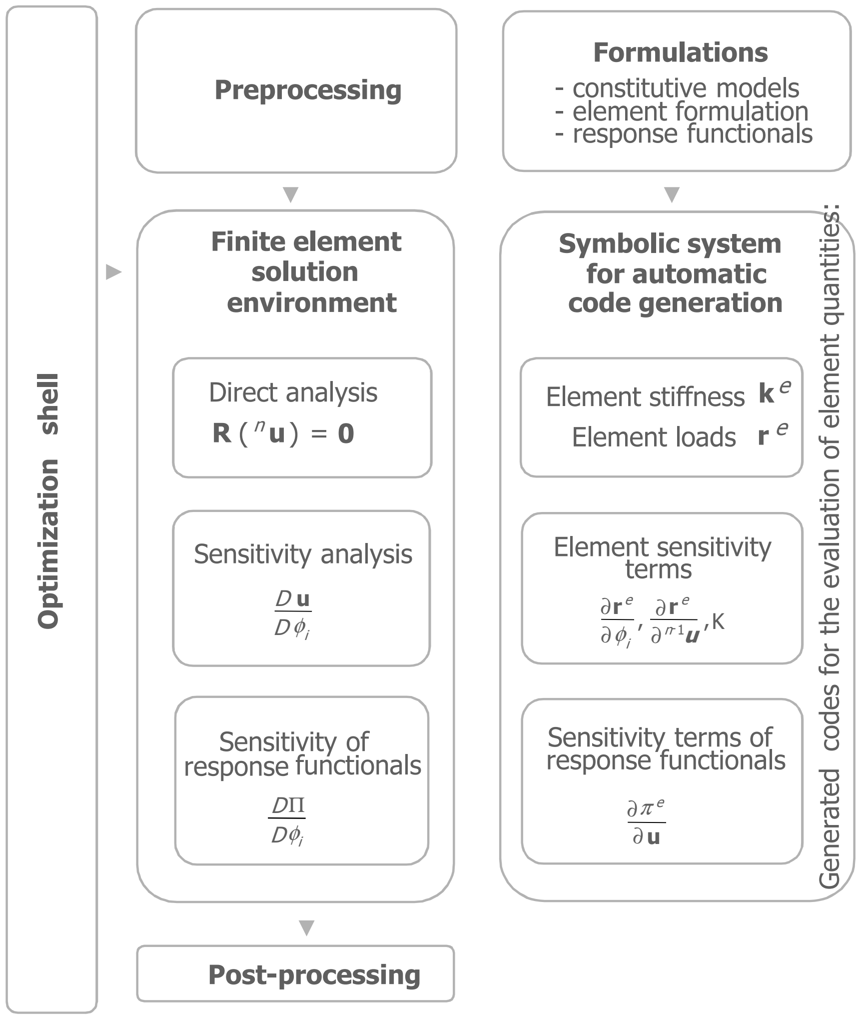

Mechanical forming of shaped cans

Polymer coated sheets

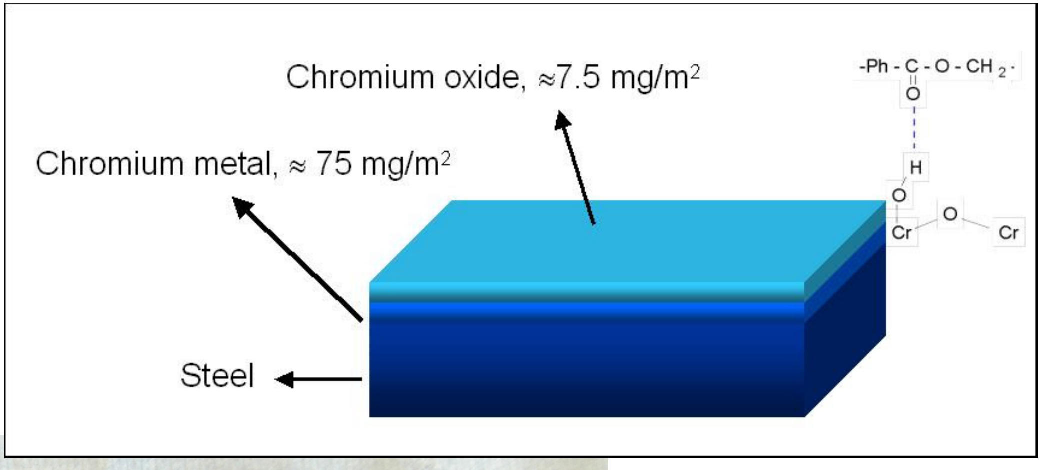

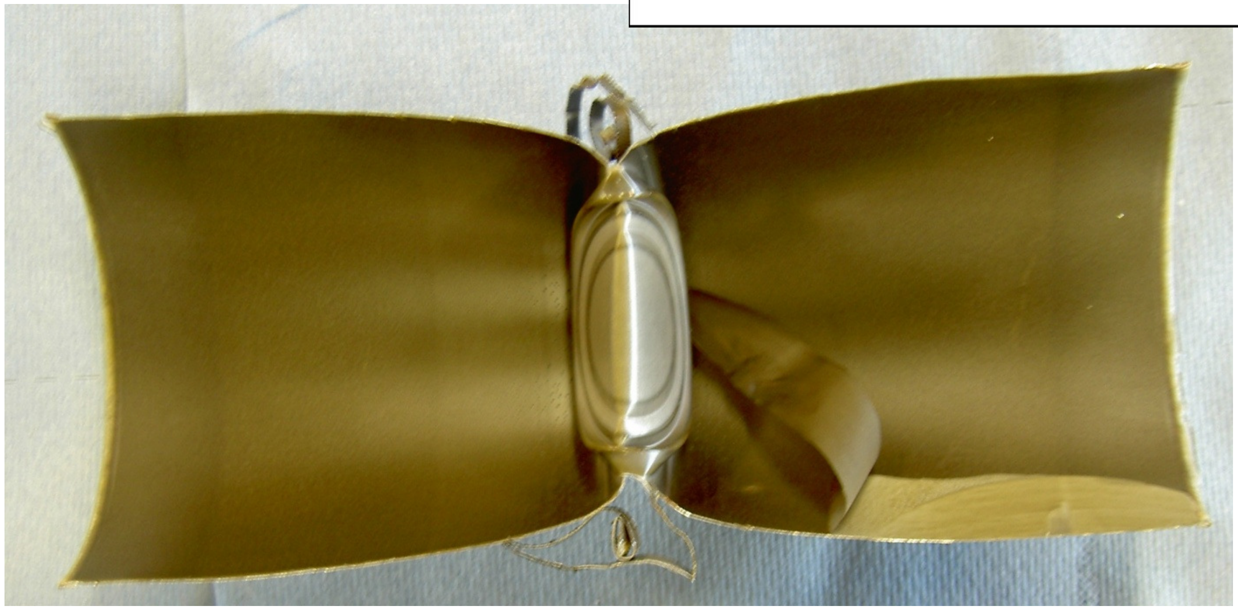

Saline test performance of polymer coated cans

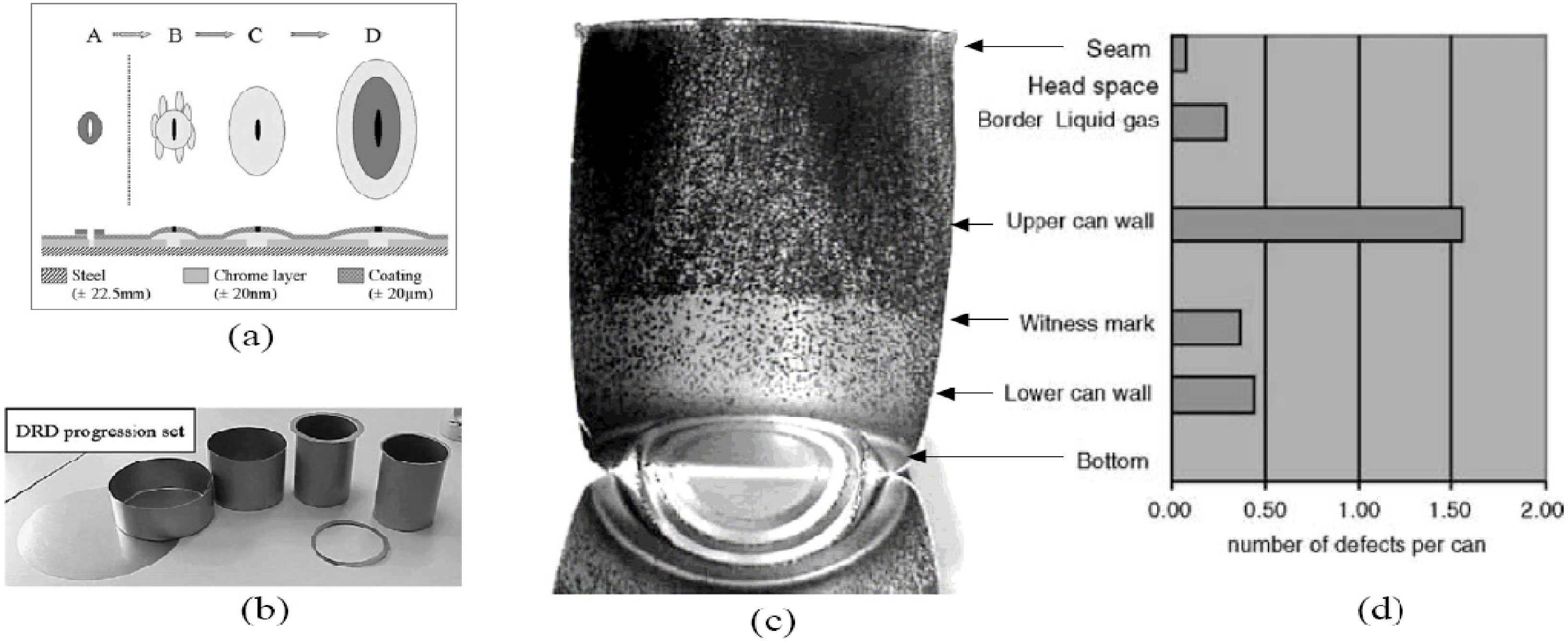

(a) (b) (c) (d)

Technological problems

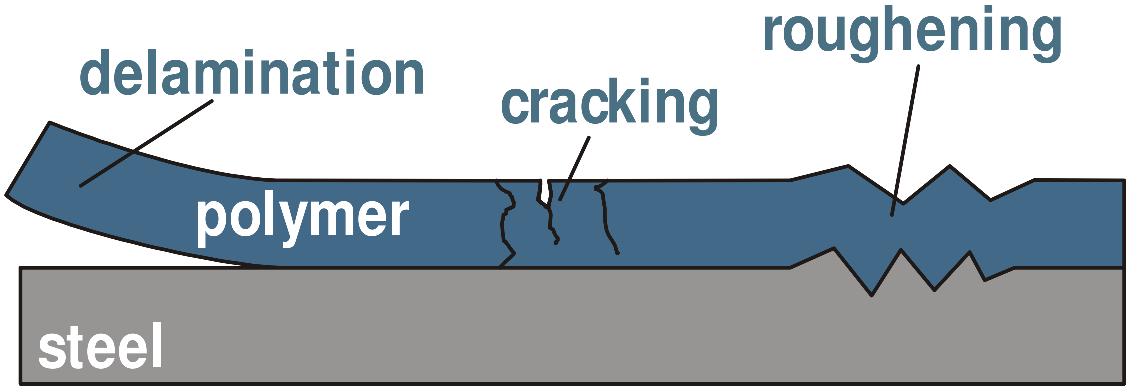

$$\sigma_{kk}(t,\mathbf{r}) = 3\int_0^t K\left[t'(t,\mathbf{r}) - \lambda'(t,\mathbf{r})\right]\frac{\partial\theta(\lambda,\mathbf{r})}{\partial\lambda}d\lambda \qquad S_{ij}(t,\mathbf{r}) = 2\int_0^t G\left[t'(t,\mathbf{r}) - \lambda'(t,\mathbf{r})\right]\frac{\partial e_{ij}(\lambda,\mathbf{r})}{\partial\lambda}d\lambda$$

K … bulk modulus , G … shear relaxation modulus, t' … material time

$$t'(t,\mathbf{r}) - \lambda'(t,\mathbf{r}) = \int_\lambda^t \frac{d\xi}{\Phi\left[T(\xi,\mathbf{r}),\theta(\xi,\mathbf{r})\right]}$$

$$\log\Phi\left[T(\xi,\mathbf{r}),\theta(\xi,\mathbf{r})\right] = \frac{b}{2.303}\left\{\frac{1}{f\left[T(\xi,\mathbf{r}),\theta(\xi,\mathbf{r})\right]} - \frac{1}{f_0}\right\}$$ … shift function

$$f\left[T(\xi,\mathbf{r}),\theta(\xi,\mathbf{r})\right]$$ … intermolecular volume

$$f\left[T(\xi,\mathbf{r}),\theta(\xi,\mathbf{r})\right] = f_0 + f_T + f_\theta$$

M … bulk creep complience , α … thermal expansion

$$f_T = \int_0^t \alpha(t-\lambda,\mathbf{r})\frac{\partial T(\lambda,\mathbf{r})}{\partial\lambda}d\lambda \qquad f_\theta = \int_0^t M(t-\lambda,\mathbf{r})\frac{\partial\sigma_{kk}(\lambda,\mathbf{r})}{\partial\lambda}d\lambda$$

Knauss WG, Emri IJ. Non-Linear Viscoelasticity based on Free-Volume Consideration, Computers & Structures, 13(1-3): 123-128 1981.
Knauss WG, Emri I. Volume Change and the Nonlinearly Thermoviscoelastic Constitution of Polymers, Polymer Engineering and Science, 27(1): 86-100 1987.

Molecular dynamics: silane molecules on the surface of zinc oxide

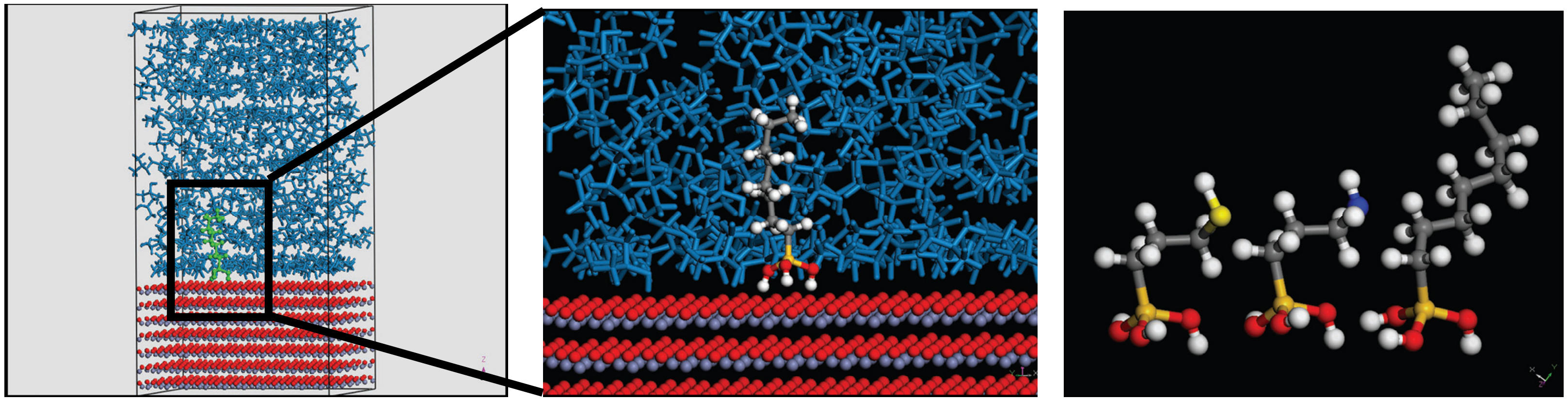

(a) (b) (c)

Accelrys Materials Studio 3.0, Accelrys Software, Inc.: San Diego, http://www.accelrys.com/products/mstudio/

A. Kornherr, S. Hansal, W.E.G. Hansal, G.E. Nauer, and G. Zifferer, Molecular dynamics simulations of the first steps of the formation of polysiloxane layers at a zinc oxide surface, Macromol. Symp., 2004, 217, 295-300.

S. Kisin, J. Bozovic Vukic, P.G.Th. van der Varst, G. de With & C.E. Koning Estimating the Polymer-Metal Work of Adhesion from Molecular Dynamics Simulations, *Chem. Mater.* 2007, *19,* 903-907

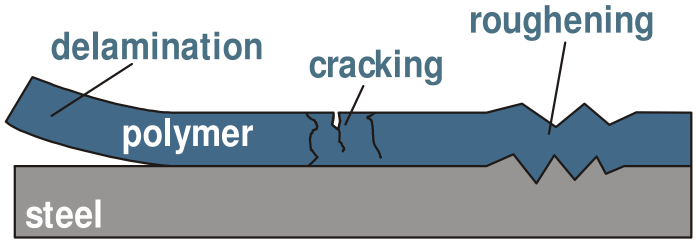

Preoblikovanje polimerno-kovinskih laminatov

Can manufacturing

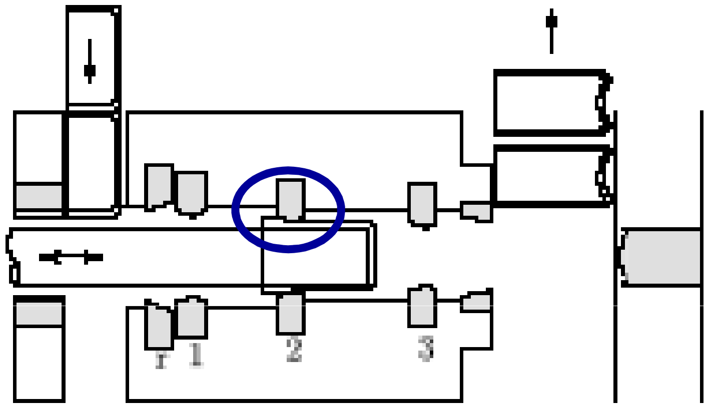

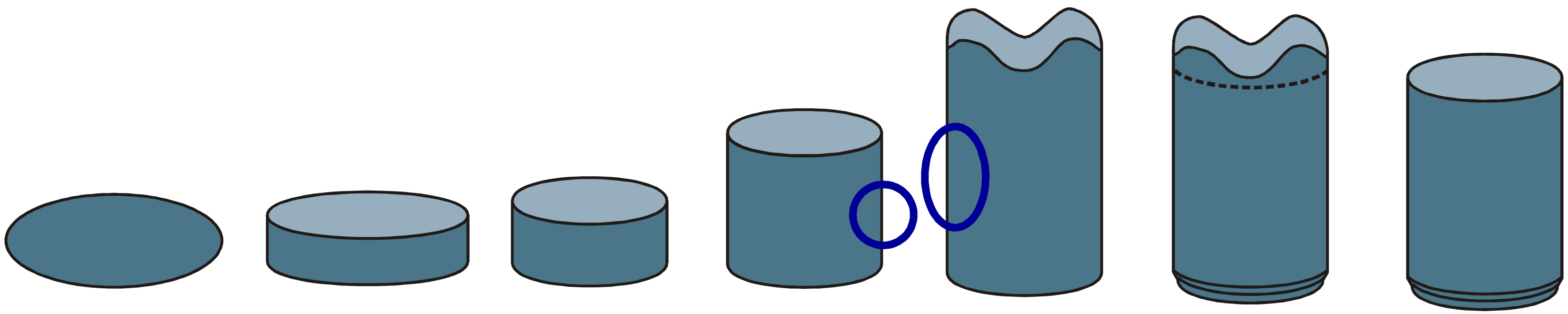

25°C

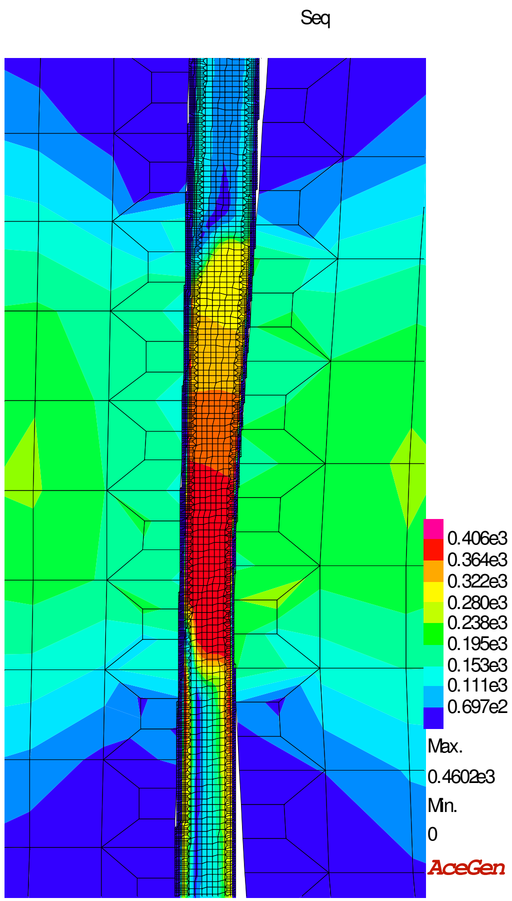
Seq
0.406e3
0.364e3
0.322e3
0.280e3
0.238e3
0.195e3
0.153e3
0.111e3
0.697e2
Max.
0.4602e3
Min.
0
AceGen

60°C

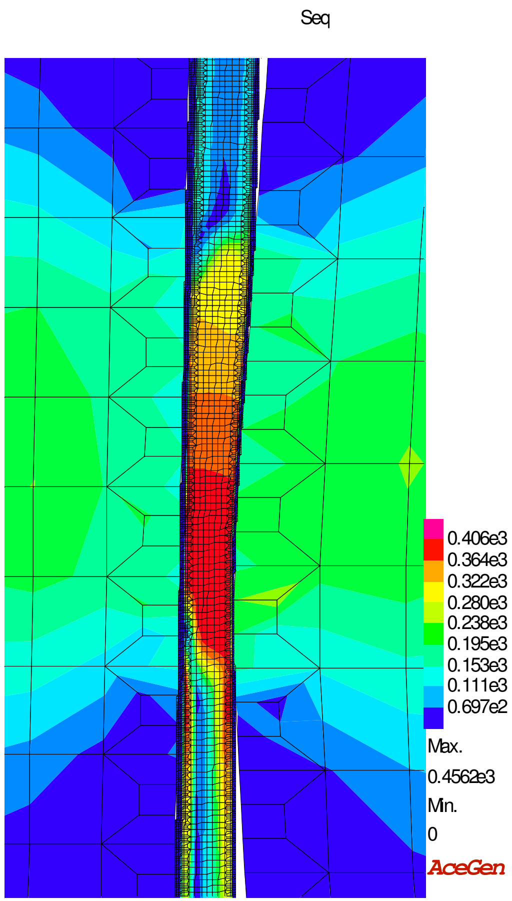
Seq
0.406e3
0.364e3
0.322e3
0.280e3
0.238e3
0.195e3
0.153e3
0.111e3
0.697e2
Max.
0.4562e3
Min.
0
AceGen

90°C

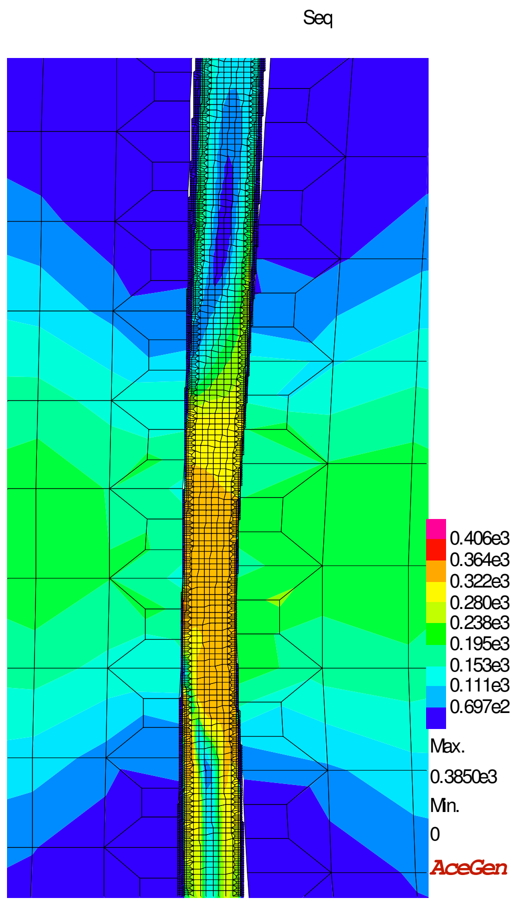
Seq
0.406e3
0.364e3
0.322e3
0.280e3
0.238e3
0.195e3
0.153e3
0.111e3
0.697e2
Max.
0.3850e3
Min.
0
AceGen

Axial force measurements

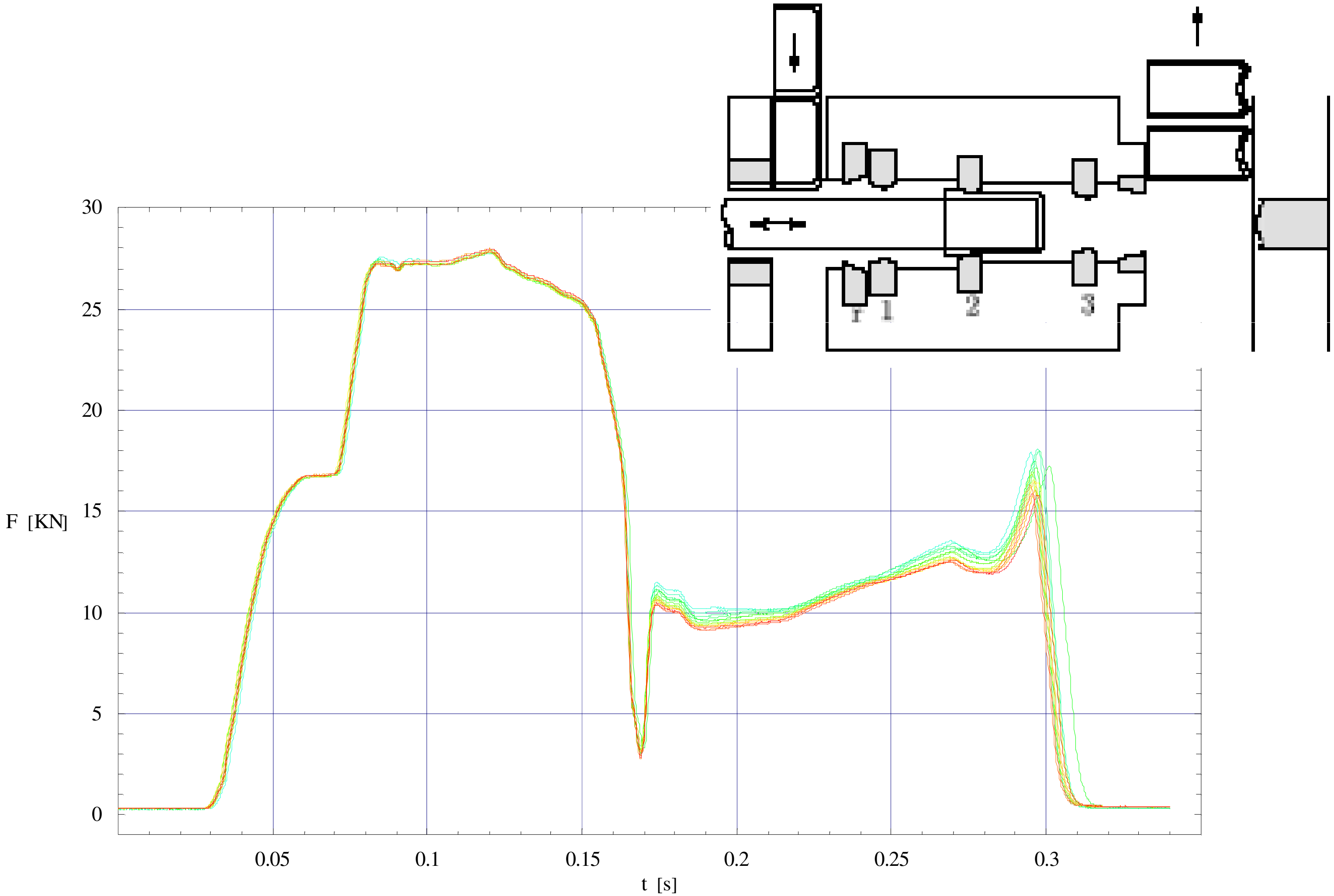

Predicted temperature increase for different production speeds

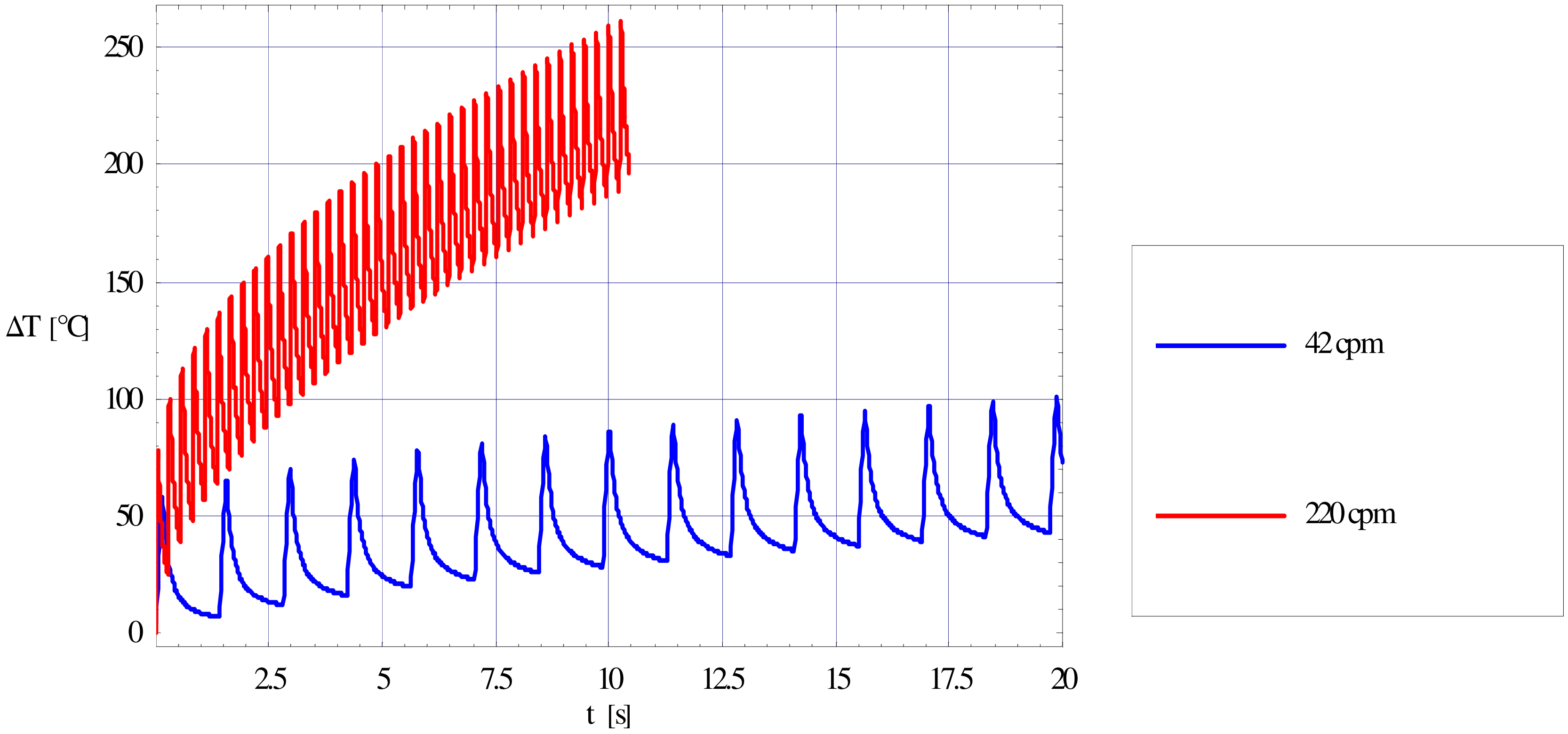

Estimated temperature increase in PET at the ring side

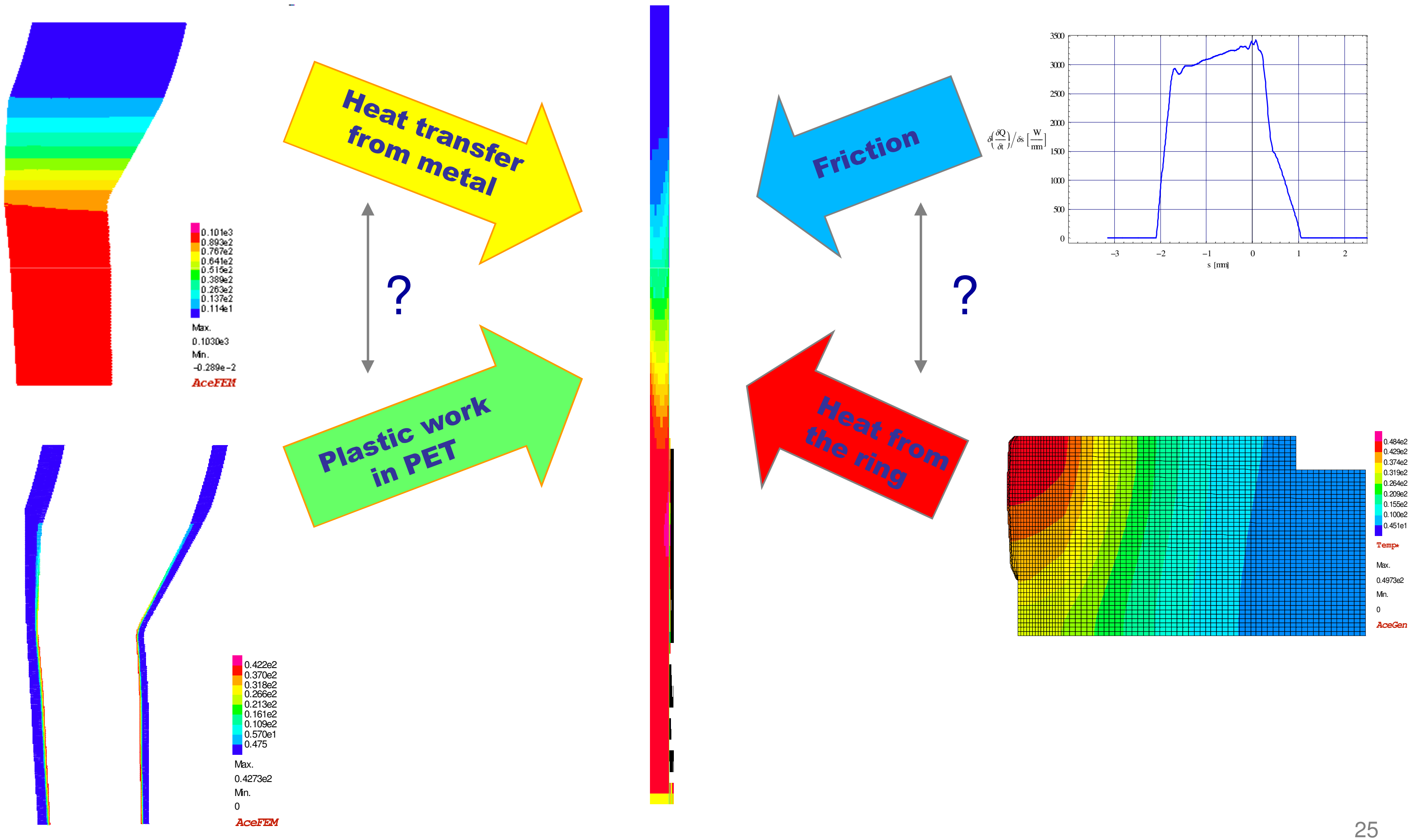

M5 modelling of the Cofiplast stone cutting process

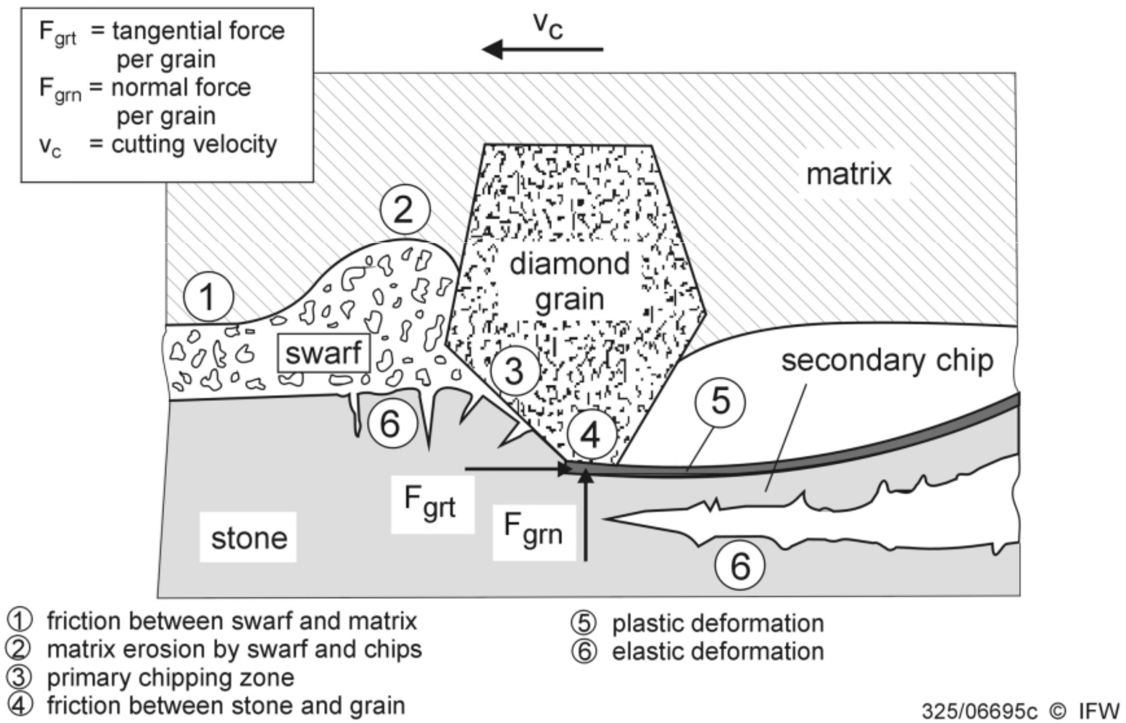

H.K. Tönshoff, H. Hillmann-Apmann, J. Asche, Diamond tools in stone and civil engineering industry: cutting principles, wear and applications, Diamond and Related Materials 11 (2002) 736–741

M5 modelling of the Cofiplast stone cutting process

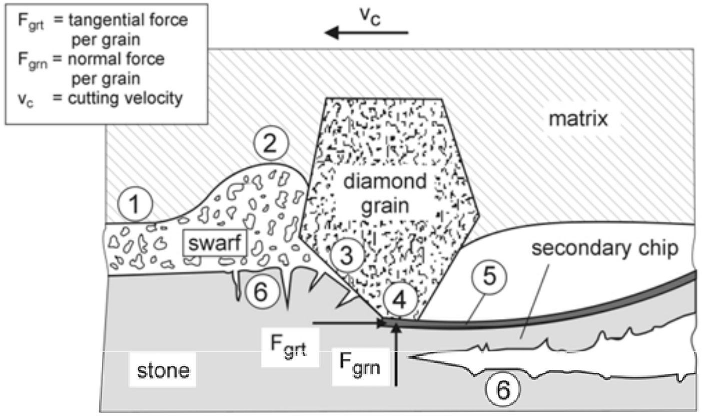

Heat transfer (FEM)

- Modeling of dissipation processes

Fluid simulations (FVM)

- Flow phenomena in the bit-stone area
- Estimates of aquaplaning effects

Macroscopic modeling of friction and abrasion

- Contact forces by Striebeck friction law
- Abrasion by Archard law

Micro mechanical modeling and analysis of cutting process (DEM)

- DE analysis with rigid particles in elastic potential
- DE analysis with elasto-plastic finite elements

Flow Analysis – Velocity Profile

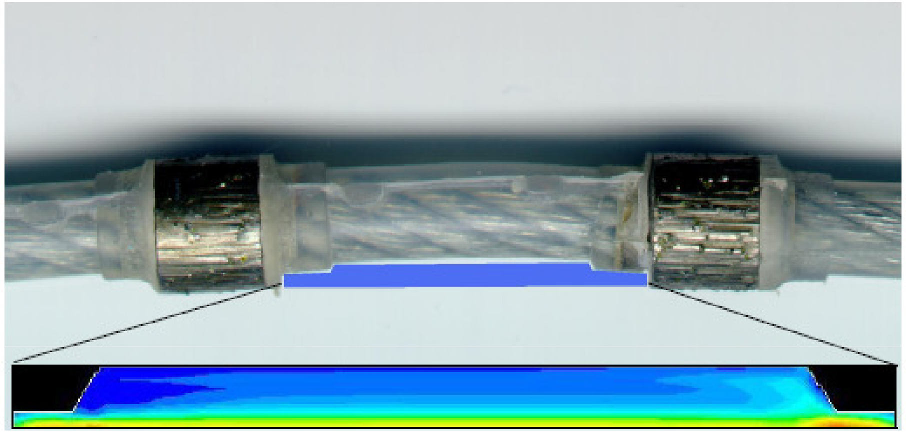

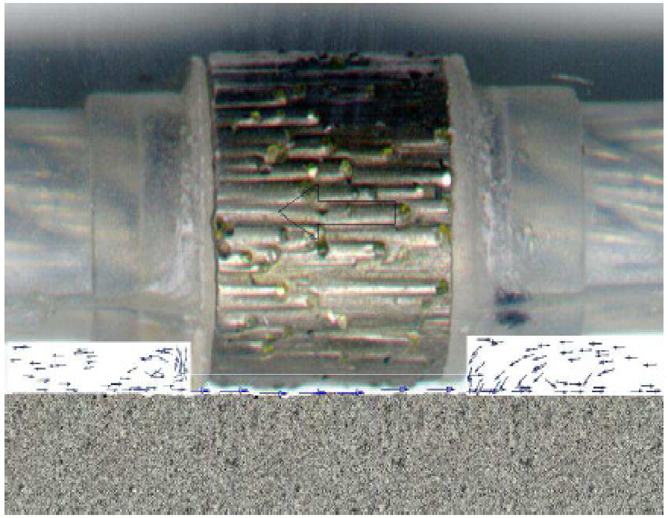

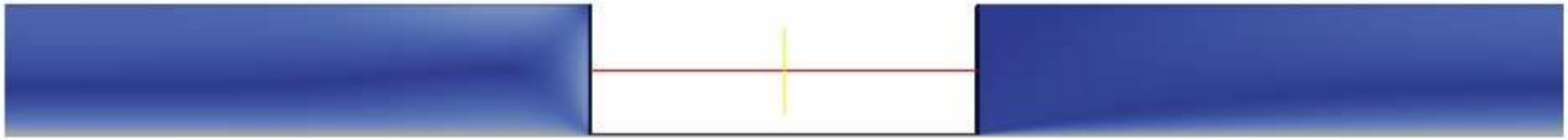

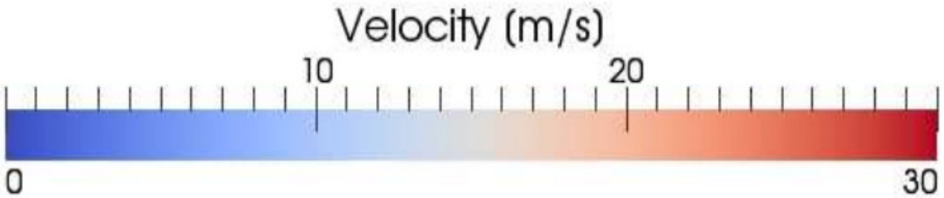

Meso-scale model of cutting process

- Geometry and SEM pictures of the structure and associated FEM model

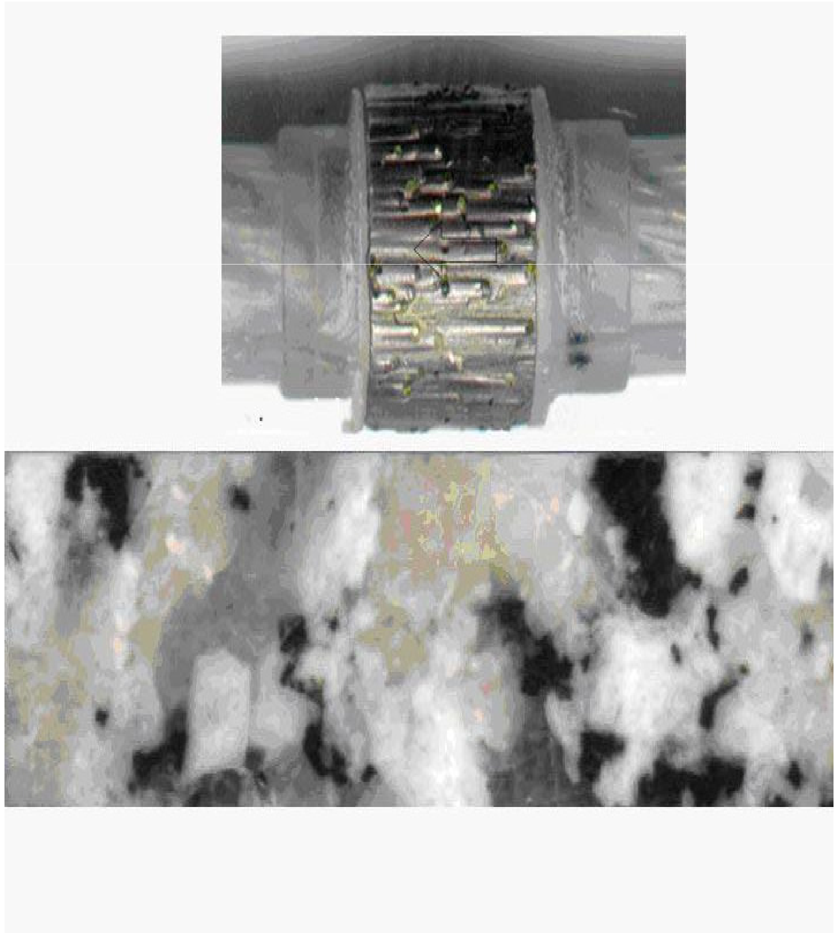

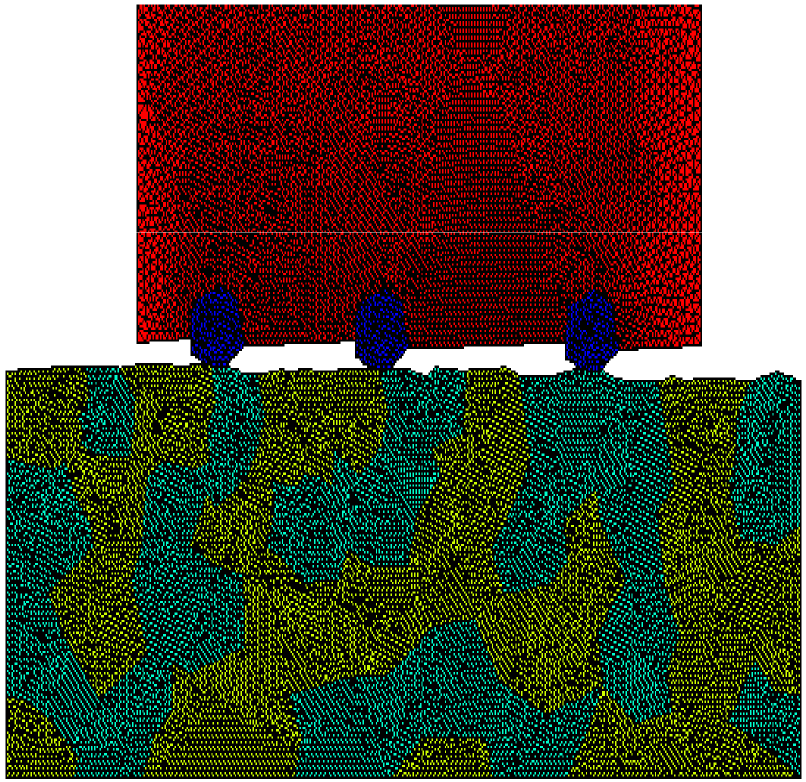

Micro-scale cutting model – FEM-DEM with rigid body particles

- **Model:**
  - **- Particle dynamics: Newtonian law of motion**
  - **- Particles contact: elastic potential with treshold spring rupture distance**

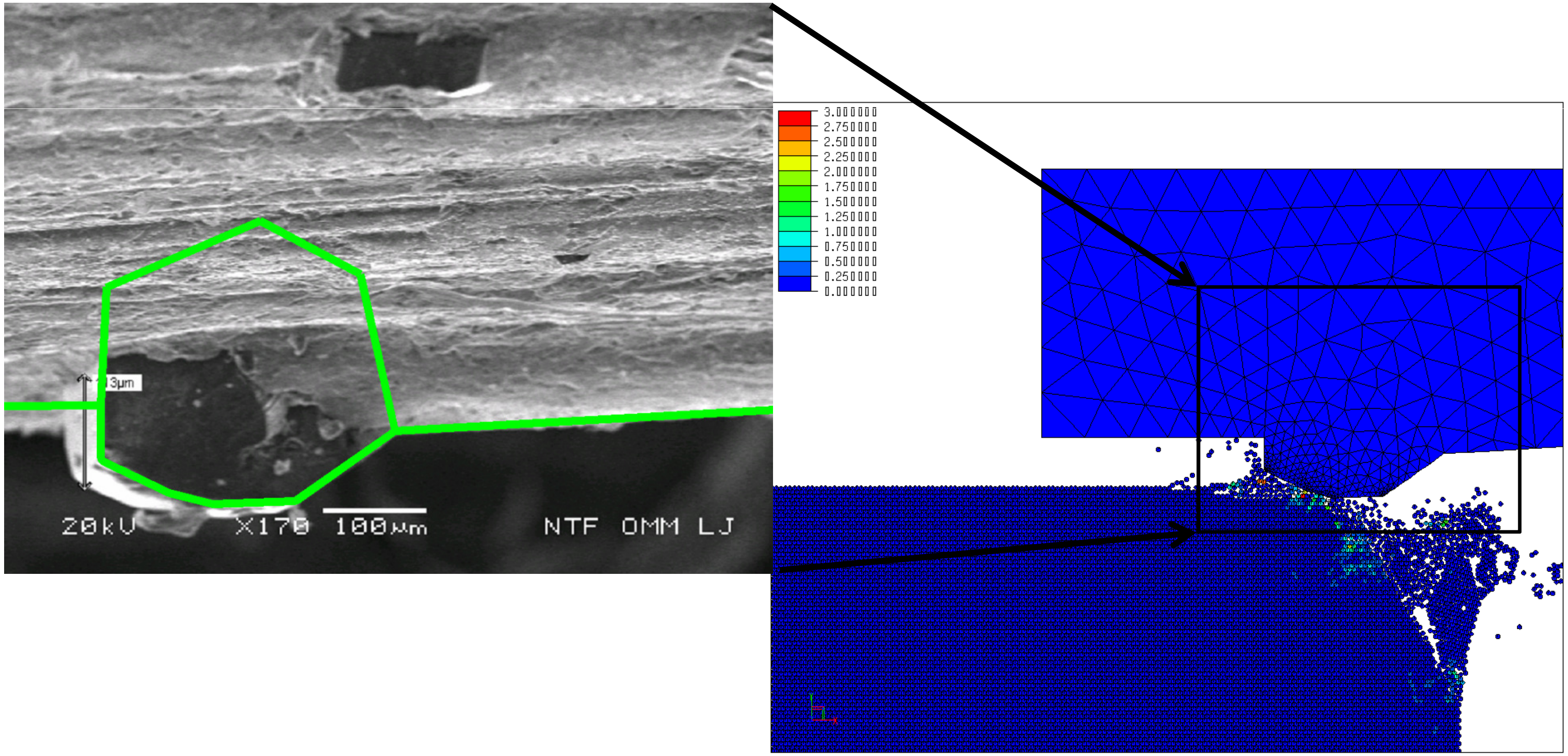

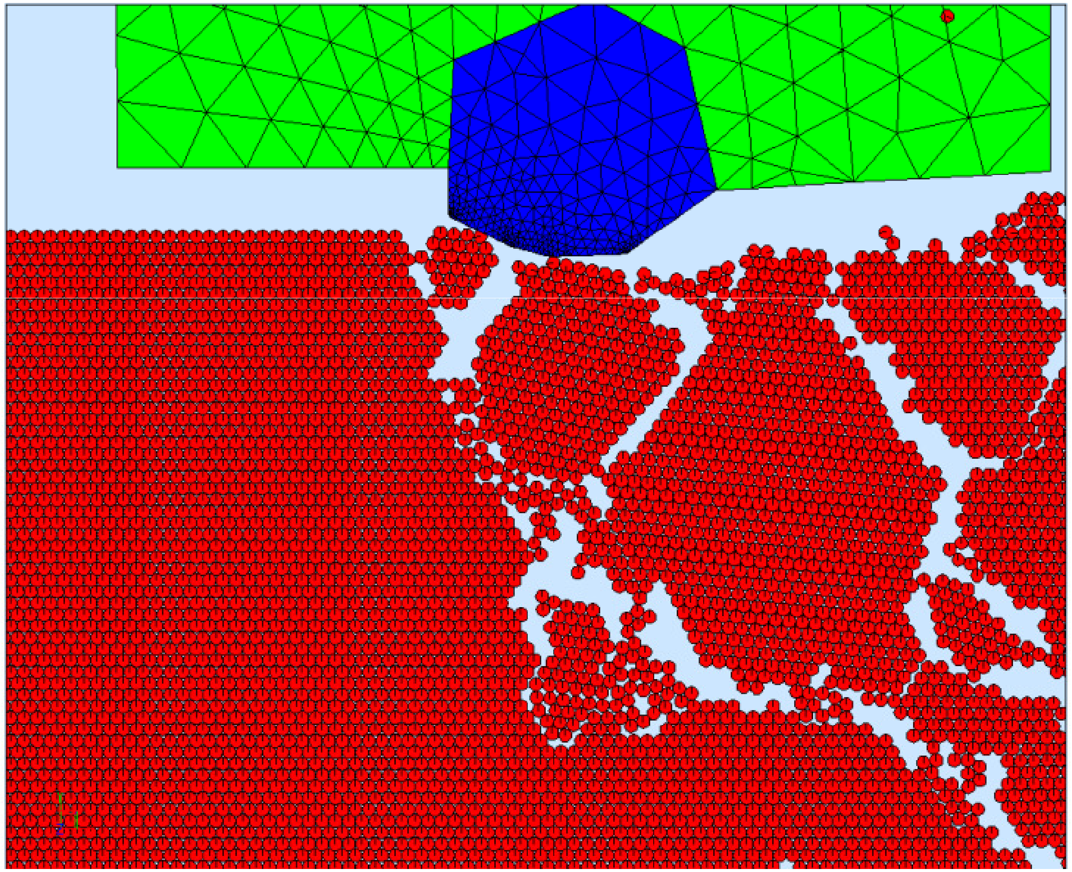

Figure 21: Effect of adhesion parameter on the cutting depth. In this case the adhesion parameter was set too low and the material is too brittle, resulting in very deep crack growth which would lead to extremely fast cutting.

Deagglomeration of nano-particles

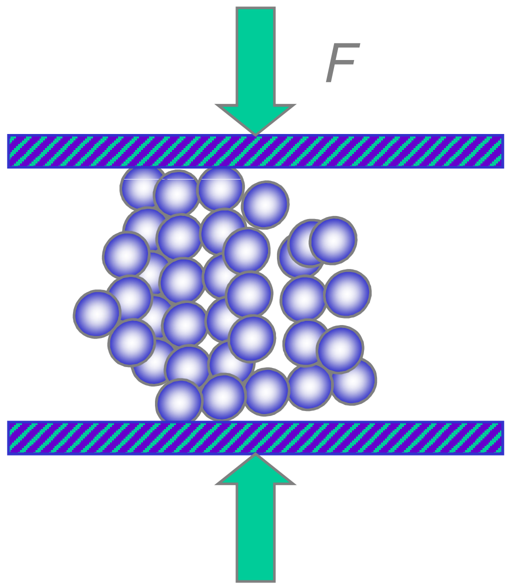

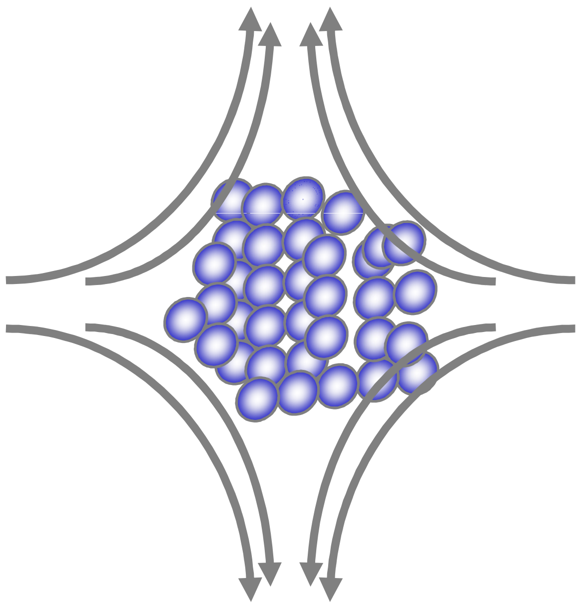

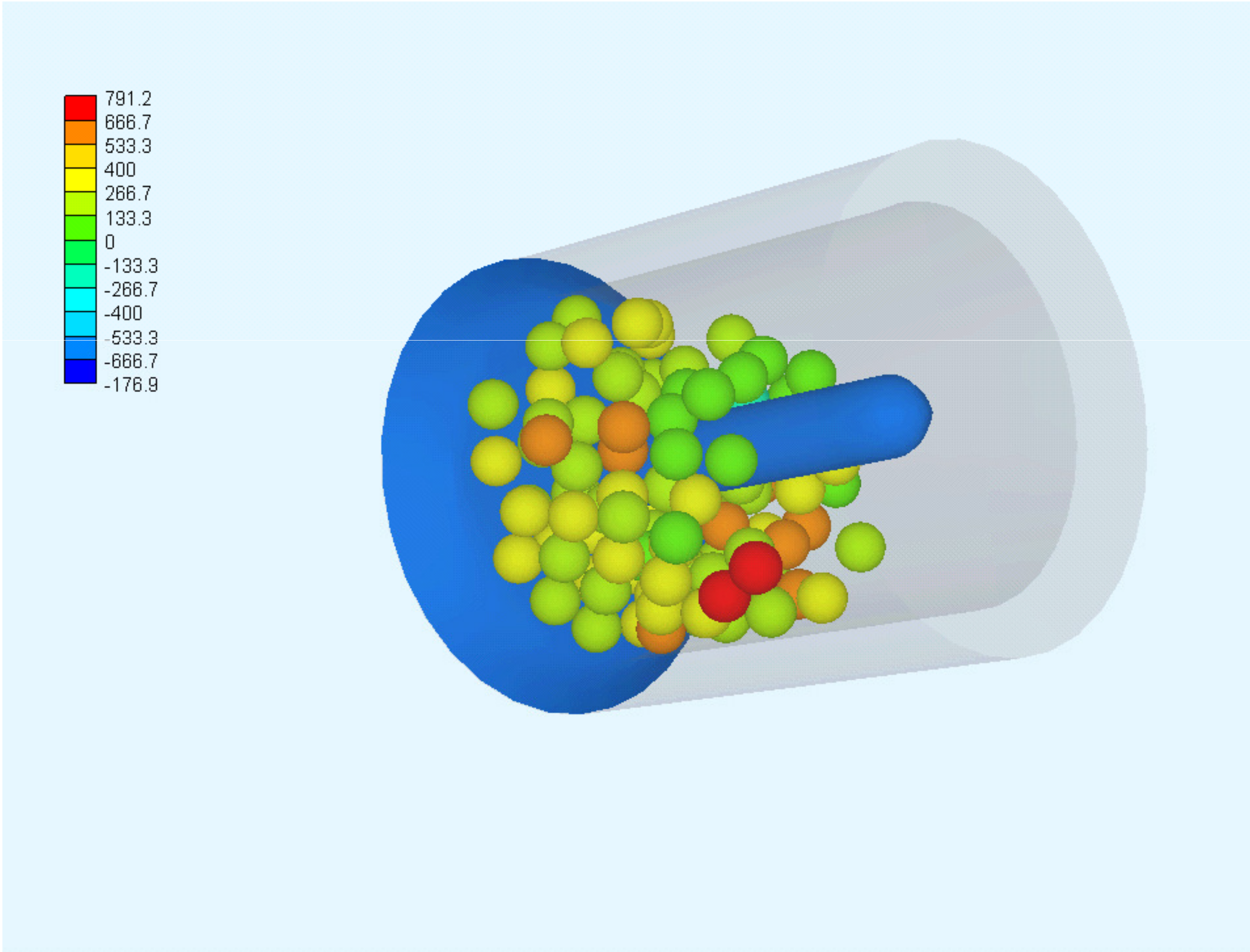
791.2
666.7
533.3
400
266.7
133.3
0
-133.3
-266.7
-400
-533.3
-666.7
-176.9

Multi-scale model

Micro –breakage mechanisms

Macro - impact scenarios

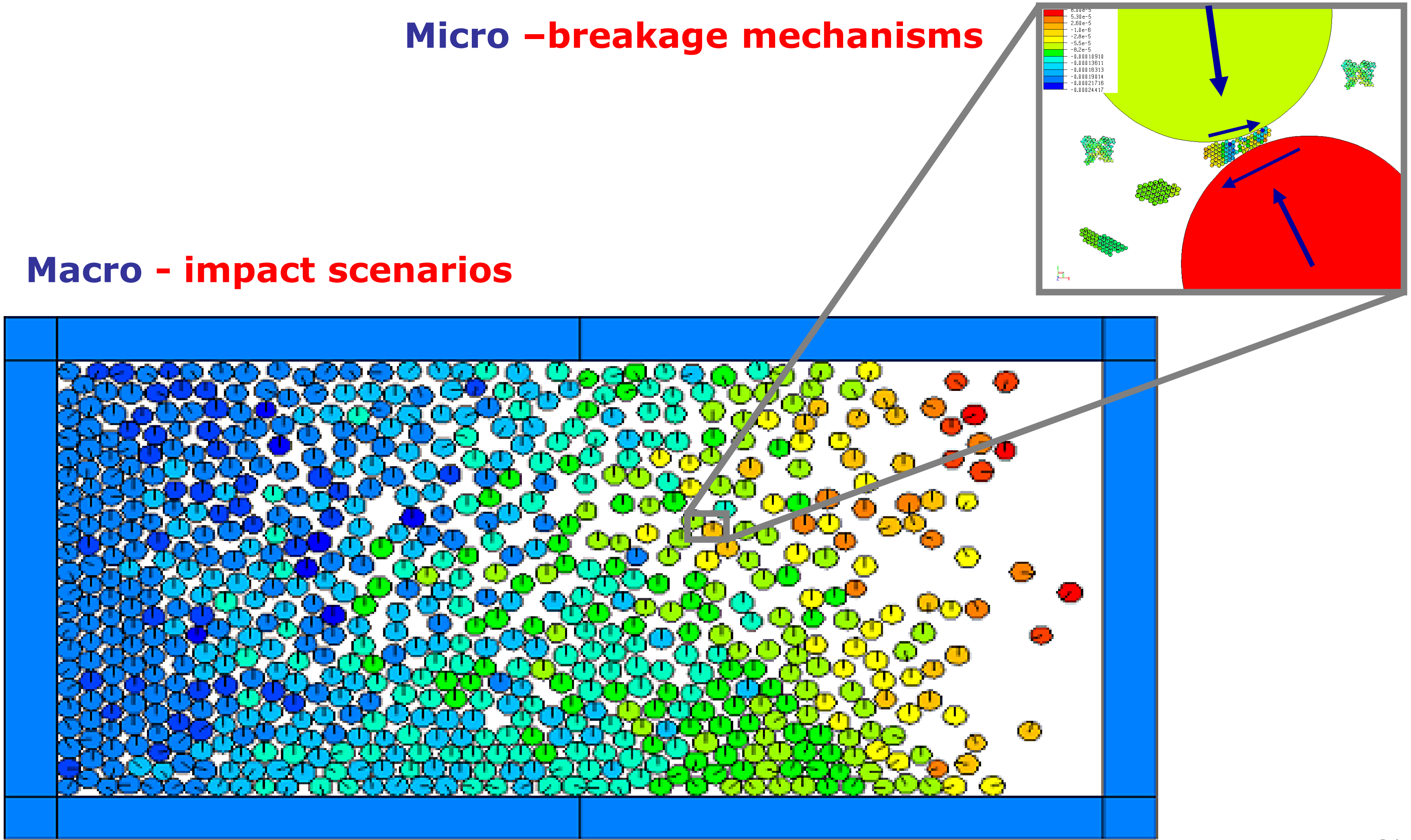

Grinding media impact statistics

	Filling ratio 70 %	Filling ratio 90%
Process design	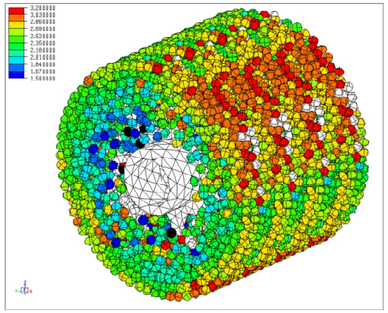	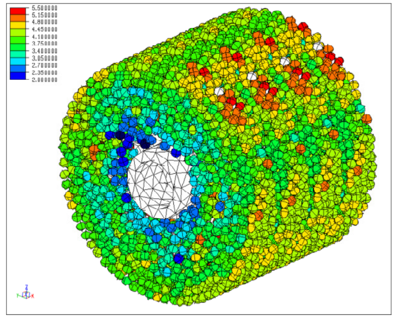
Beads velocity	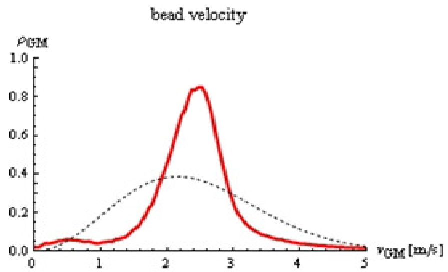	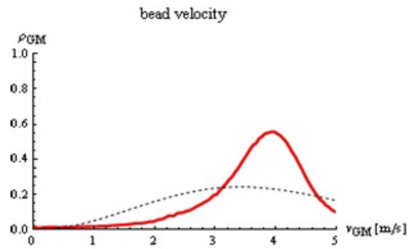
Impact velocity and angle	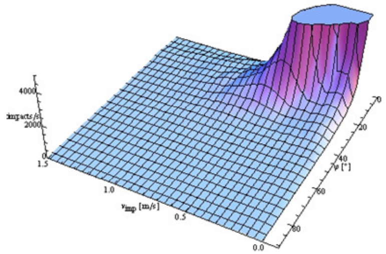	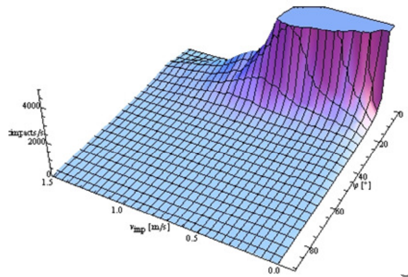

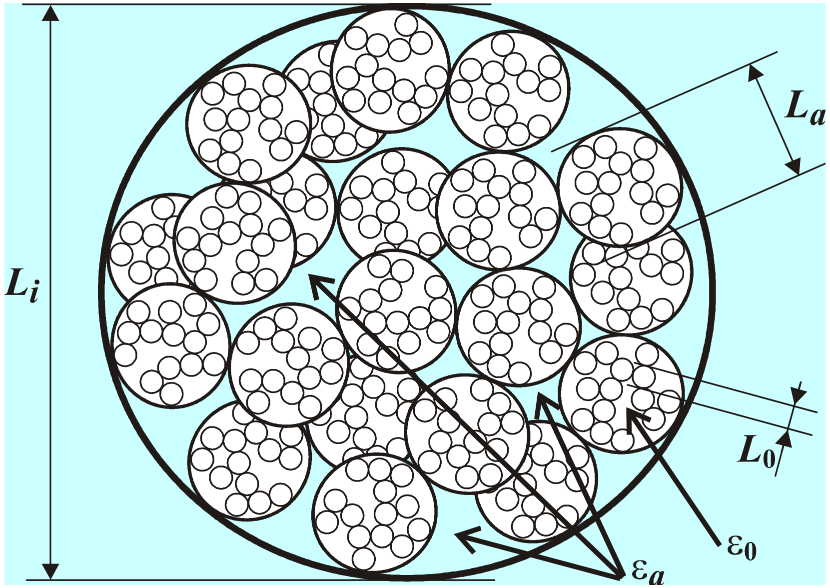

Structure of large agglomerates

Inter-molecular distance	2.0×10^{-10} m
Hamaker Constant	8.5×10^{-19}
Elementary charge of the proton	1.6×10^{-19}
Ion concentration in the solution	1.0×10^{-29}
Surface potential	0.015 mV
Debye screening parameter	1.9×10^{9}

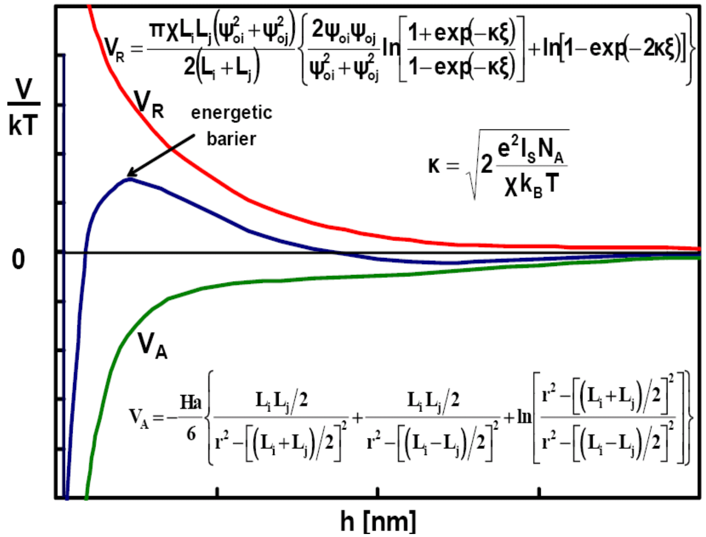

Impact analysis

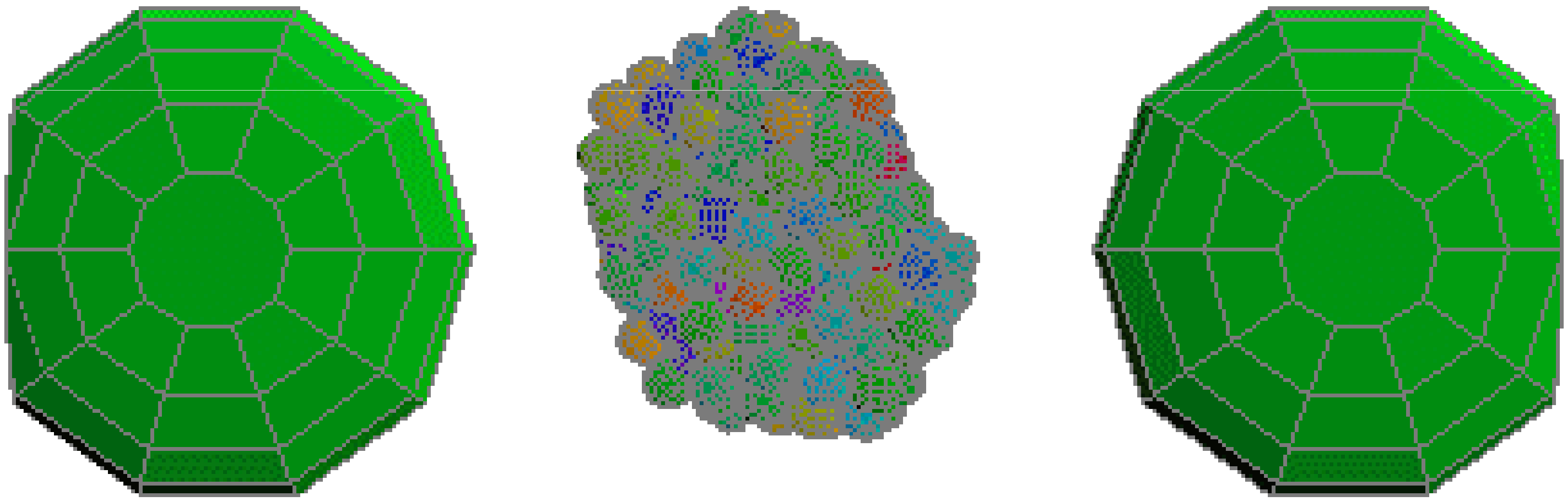

Rotor stator

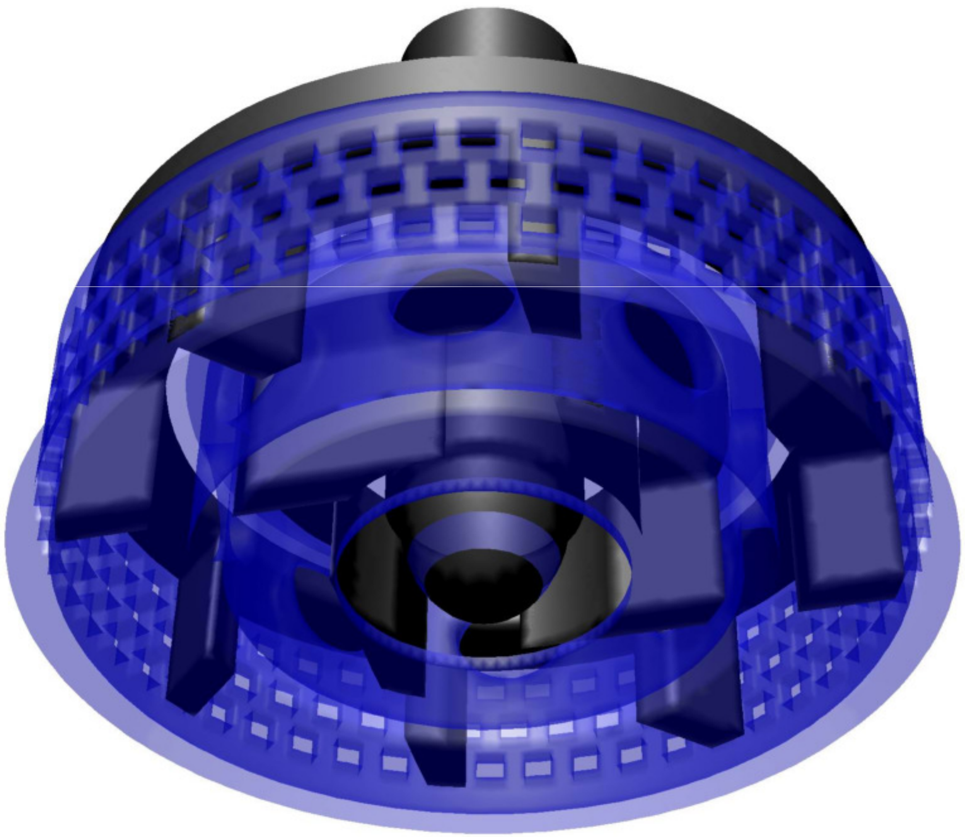

Industrijski partnerji na področju nano delcev

?

Prisma (2009)

MEMS micropropulsion for precise manoeuvring of satellites

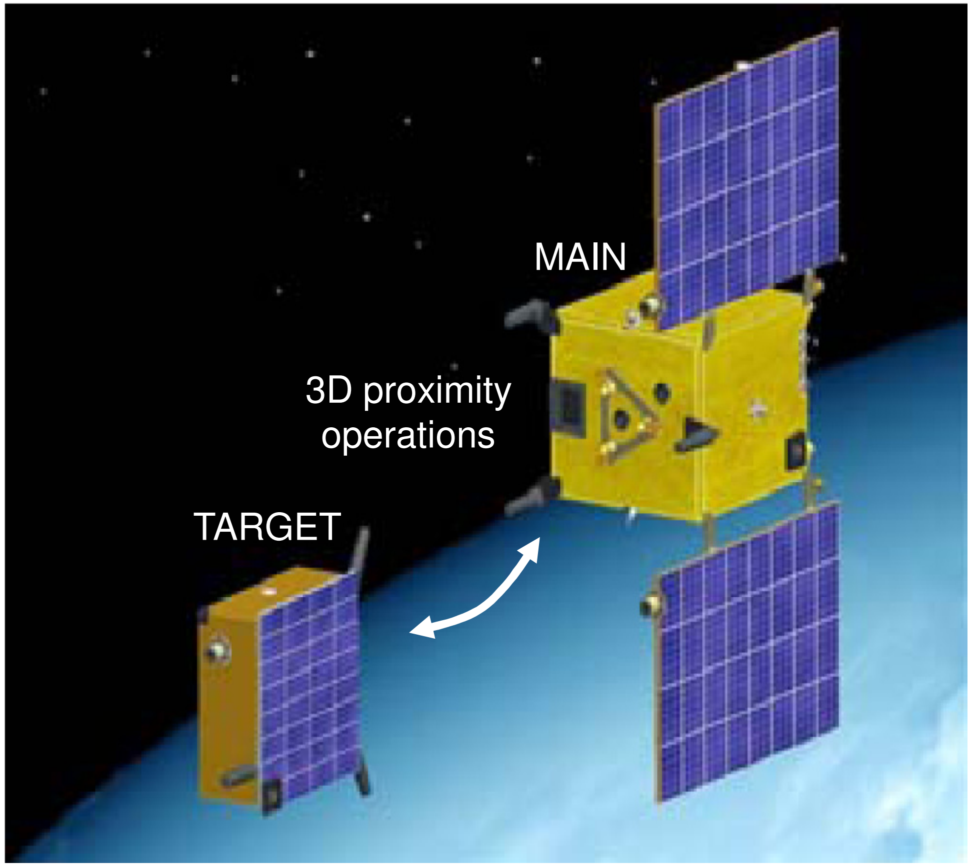

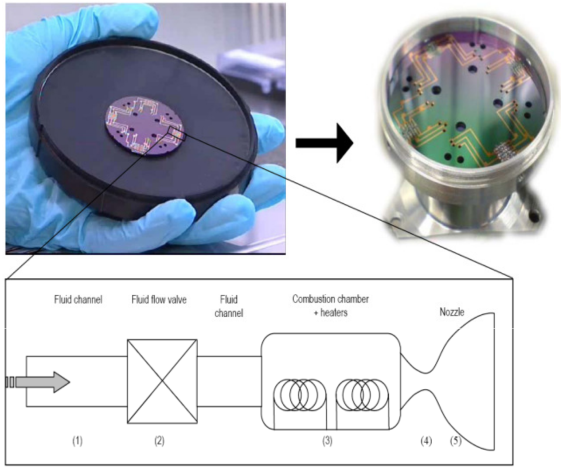

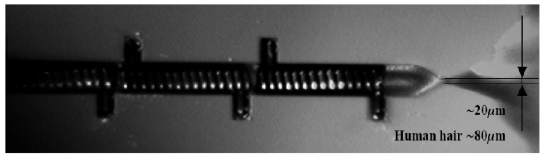

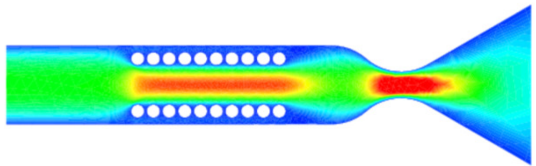

Tržno zanimivi satelitski razredi

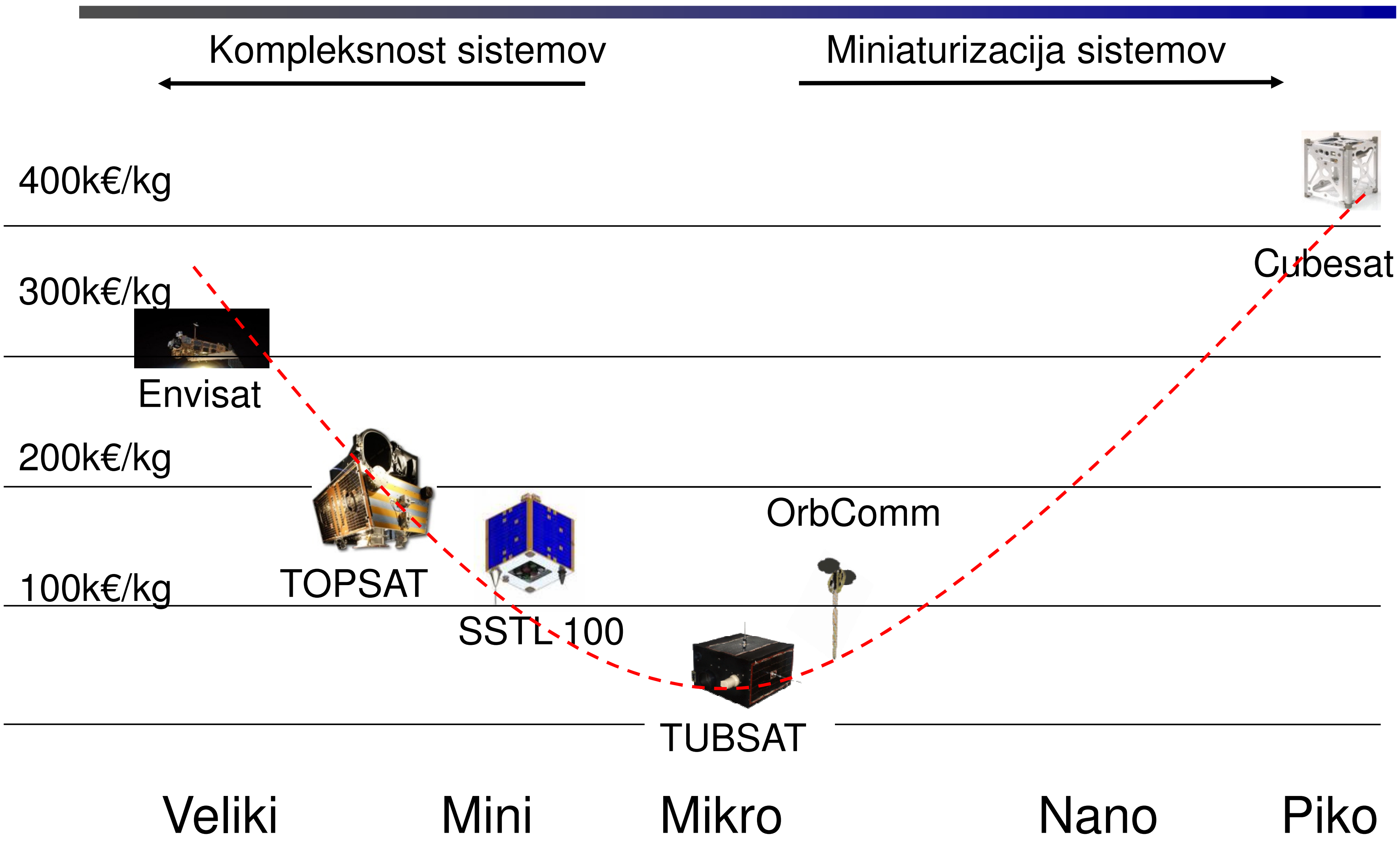

Remote sensing of Slovenia

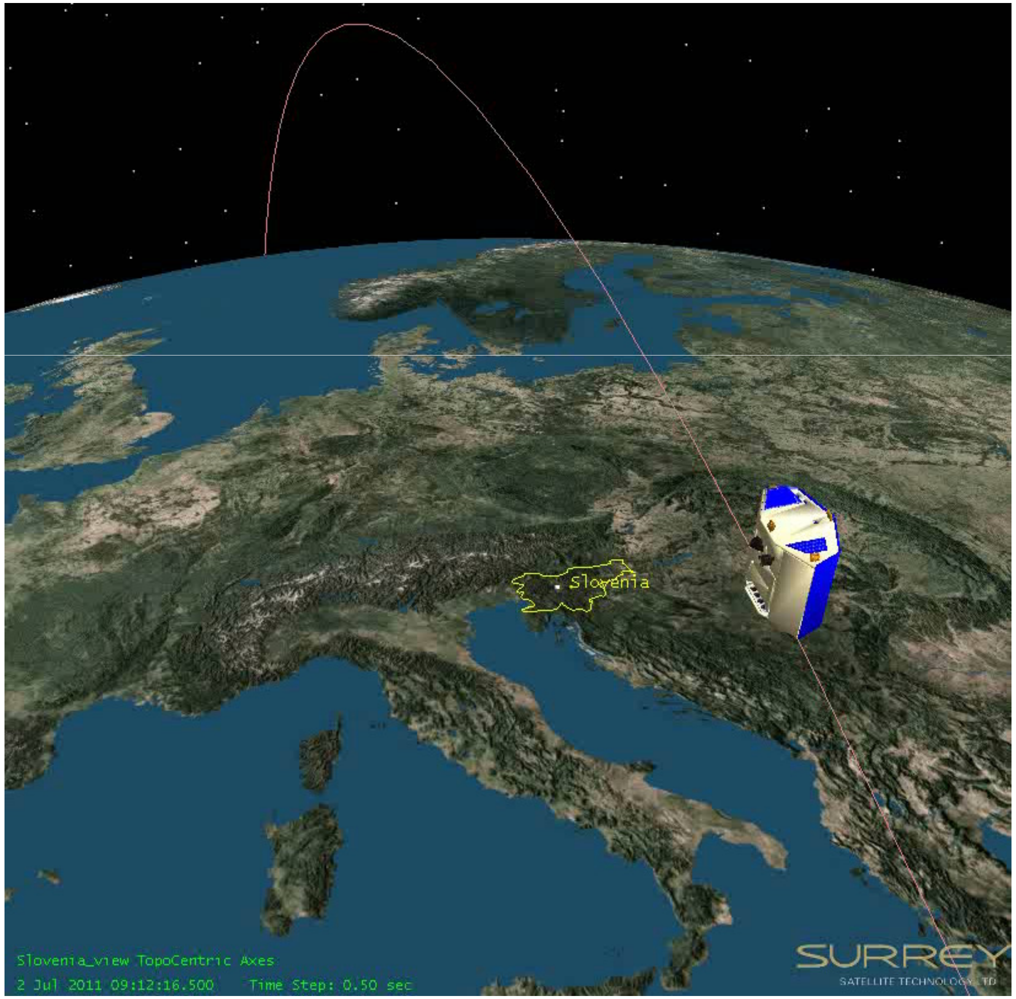

Lapan-Tubsat test

Koper, 25.6.2008

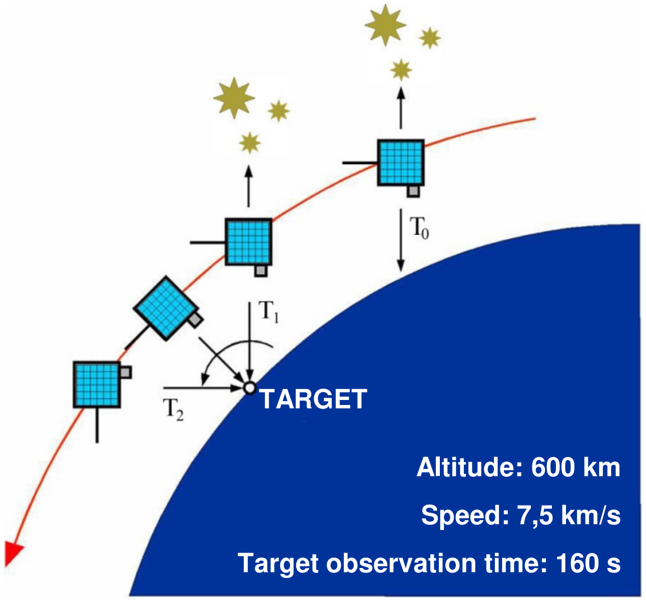

Strategija kontrole

Plane: 10km (60 times lower), 0,25 km/s (30 times slower)

M5 development vision

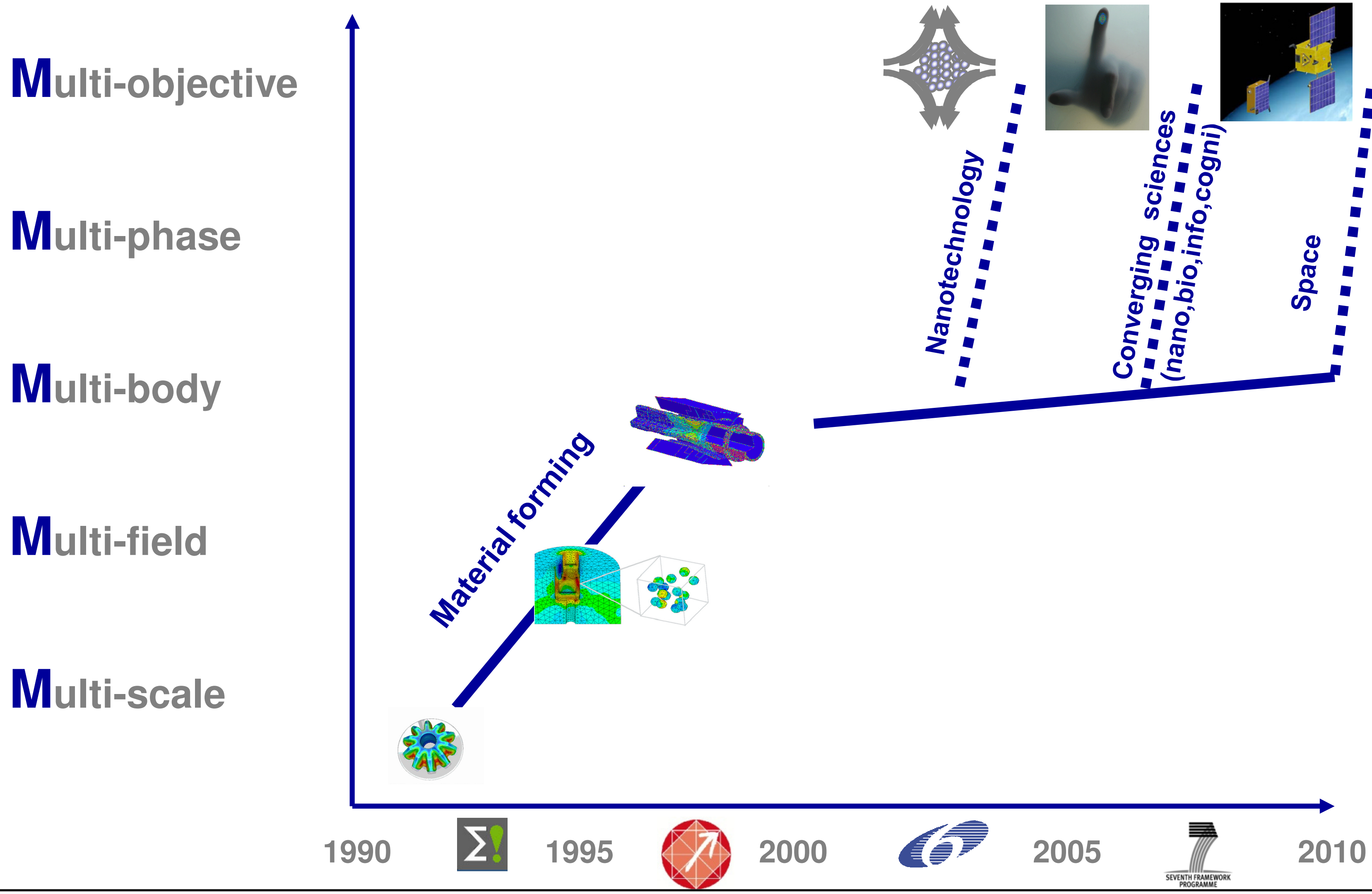

tomaz.rodic@omm.ntf.uni-lj.si